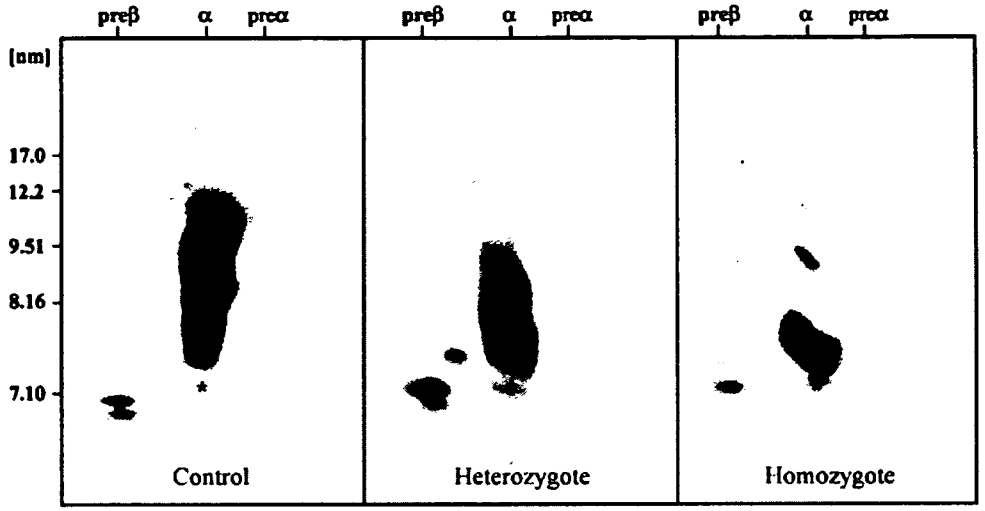

Fig. 1. Apolipoprotein A-I (apoA-I)-containing HDL subpopulations of representative control, heterozygous, and homozygous LCAT-deficient subjects separated by two-dimensional, nondenaturing agarose-PAGE. The asterisk represents the endogenous human serum albumin marking the α-mobility front.

TG (−7%) values compared with controls. Homozygotes had about 1% of the LCAT activity and about 23% of the LCAT mass of controls. They had significantly lower HDL-C (−83%), apoA-I (−76%), apoA-II (−71%), apoB (−68%), and LDL-C (−49%), and 48% higher TG values than controls.

Figure 1 and **Table 2** summarize data on apoA-I-containing HDL subpopulations in controls and in heterozygous and homozygous LCAT-deficient subjects. Heterozygotes had one extra particle in the preβ-1 region (preβ-1×); however, all of their other apoA-I-containing HDL subpopulations were comparable to controls in electrophoretic mobility and size. ApoA-I distribution in heterozygotes was shifted toward the smaller HDL particles: there was a 2-fold increase in preβ-1 level, a 23% increase in α-4, and a 45% increase in preα-4 levels compared with controls. There were significant decreases in the concentrations of all the other HDL particles, whereas the mean concentration of α-3, an intermediate-sized particle, was similar to that of controls. In homozygotes, the majority of apoA-I was detected in small, lipid-poor, disc-shaped HDL particles (preβ-1 and α-4). Despite the low plasma concentrations of apoA-I in homozygous subjects, the apoA-I concentrations of these particles were comparable to those of controls. We have also observed larger (~8 nm–20 nm) apoA-I-containing HDL particles with α-mobility in many of the homozygotes. **Figure 2** represents the distribution of apoA-II-containing particles—superimposed on apoA-I-containing particles—in representative control, heterozygous, and homozygous LCAT-deficient subjects. In control subjects, α-2 and α-3 HDL contain apoA-I and apoA-II. In heterozygotes, some apoA-II was detected in the preβ-1 region but the majority of apoA-II was distributed in the α-2 and α-3 subpopulations, with a slight shift toward the smaller α-3 particles, compared with controls. In contrast to controls, homozygotes had a very low level of apoA-II, which was detected in a small, lipid-poor particle, comigrating with the regular LpA-I preβ-1 HDL particles. Total or partial LCAT deficiency had no significant effect on the concentration of apoA-IV or the distribution of apoA-IV-containing HDL particles (**Fig. 3**). There were no significant differences between heterozygotes and controls in apoC-I concentration and distribution (**Fig. 4**). In contrast, homozygotes had significantly lower apoC-I levels, and their apoC-I was found on the top of the gel with β-mobility, indicating that apoC-I was present solely in VLDL particles, not in α-mobility HDL particles, as in controls and heterozygotes. The concentrations and distribution of apoC-III were significantly different between LCAT-deficient subjects and controls (**Fig. 5**). In controls, the majority of apoC-III comigrated with apoA-I in α-1 and α-2 HDL, and some was also found

TABLE 2. Concentrations of HDL subpopulations as determined by apoA-I content

	Controls (n = 22)	Heterozygotes (n = 11)	Homozygotes (n = 11)
Preβ-1_x	Not detectable	0.7 ± 0.9*	1.6 ± 1.0*
Preβ-1_a	8.2 ± 3.2	14.6 ± 5.4*	7.9 ± 4.0
Preβ-1_b	4.1 ± 1.6	10.3 ± 8.1*	1.8 ± 1.1*
Preβ-2_a	0.7 ± 0.4	0.3 ± 0.2*	Not detectable
Preβ-2_b	1.0 ± 0.5	0.5 ± 0.3*	Not detectable
Preβ-2_c	0.5 ± 0.3	0.2 ± 0.2*	Not detectable
α-1	16.7 ± 8.9	11.0 ± 8.6*	
α-2	39.1 ± 9.6	25.3 ± 6.7*	11.6 ± 2.4
α-3	24.3 ± 5.6	23.2 ± 5.5	
α-4	13.4 ± 3.6	16.5 ± 3.5*	12.1 ± 7.0
Preα-1	5.2 ± 3.3	0.9 ± 0.9*	
Preα-2	6.2 ± 2.4	1.9 ± 1.1*	0.6 ± 0.4
Preα-3	3.4 ± 1.4	2.0 ± 1.0*	
Preα-4	1.1 ± 0.4	1.6 ± 0.8*	0.6 ± 1.0

Data are mean (mg/dl) ± SD.
*Significantly different ($P < 0.05$) from control.

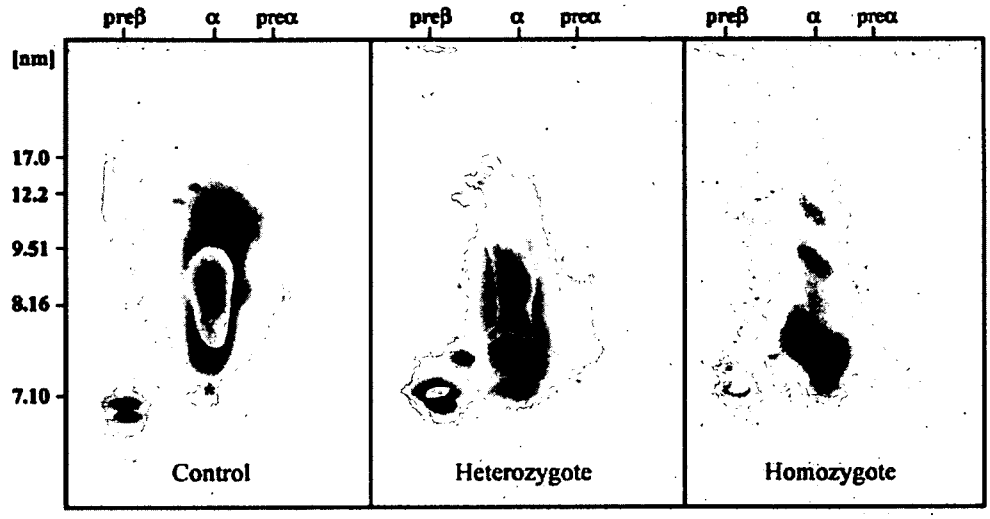

Fig. 2. ApoA-II-containing HDL subpopulations of representative control, heterozygous, and homozygous LCAT-deficient subjects superimposed on the image of apoA-I-containing subpopulations. LCAT-deficient subjects have apoA-II in small, preβ-migrating HDL particles. The asterisk represents the endogenous human serum albumin marking the α-mobility front.

in the α-3 and α-4 size range, with no comigration with apoA-I. In contrast, practically all of the apoC-III was detected in small, lipid-poor HDL particles in homozygotes and heterozygotes. ApoE-containing particles migrated with β-preβ-mobility in the size range between 12 nm and VLDL size, with a median diameter of 16.5 nm in controls (**Fig. 6**) and no overlap with apoA-I-containing HDL particles. In heterozygotes, apoE was also found in large β-preβ-mobility particles, with no comigration with apoA-I. Interestingly, the size of apoE-containing particles was somewhat increased in heterozygotes compared with controls. Homozygotes had much less apoE than controls. ApoE concentrations in the larger particles decreased, and smaller apoE-containing particles appeared in the plasma of homozygotes.

DISCUSSION

The purpose of this study was to gain insight into the role that LCAT plays in HDL metabolism as well as to better understand LCAT deficiency states. Characteriz-

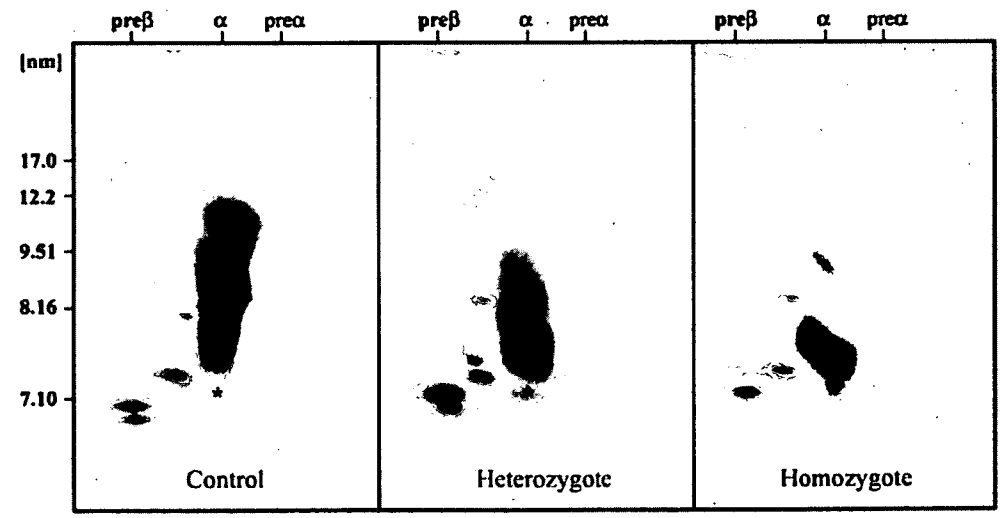

Fig. 3. ApoA-IV-containing HDL subpopulations of representative control, heterozygous, and homozygous LCAT-deficient subjects superimposed on the image of apoA-I-containing subpopulations. Total or partial LCAT deficiency has no significant effect on the distribution of apoA-IV-containing HDL particles. The asterisk represents the endogenous human serum albumin marking the α-mobility front.

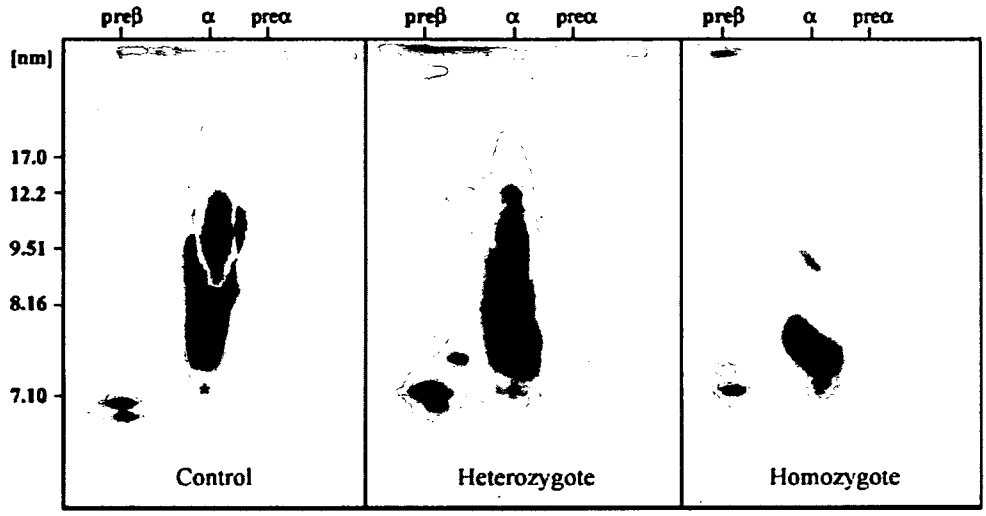

Fig. 4. ApoC-I-containing HDL subpopulations of representative control, heterozygous, and homozygous LCAT-deficient subjects superimposed on the image of apoA-I-containing subpopulations. In homozygotes, apoC-I has only been detected on the top of the gel with β-mobility (VLDL) in contrast to controls and heterozygotes. The asterisk represents the endogenous human serum albumin marking the α-mobility front.

ing HDL particles in patients with rare inborn errors of HDL metabolism has been helpful in better understanding HDL particle metabolism and reverse cholesterol transport. We have documented that Tangier disease patients had: *1*) apoA-I only in the preβ-1 HDL particles, *2*) no apoA-II-containing HDL, and *3*) decreased size of apoE HDL. ApoA-IV was not significantly influenced by the lack of ABCA1-mediated cellular cholesterol efflux (16). We have subsequently reported that HDL subpopulations in CETP-deficient homozygotes were very large, compositionally undifferentiated HDL particles (17). Therefore, CETP activity is essential for the formation of distinguished HDL particles in the normal size range of HDL. Most importantly, CETP activity is essential for the formation of discrete LpA-I, LpA-I:A-II, and LpE HDL particles.

In the present manuscript, we document the role of LCAT in HDL metabolism and remodeling in plasma. The first important observation is that LCAT activity is not

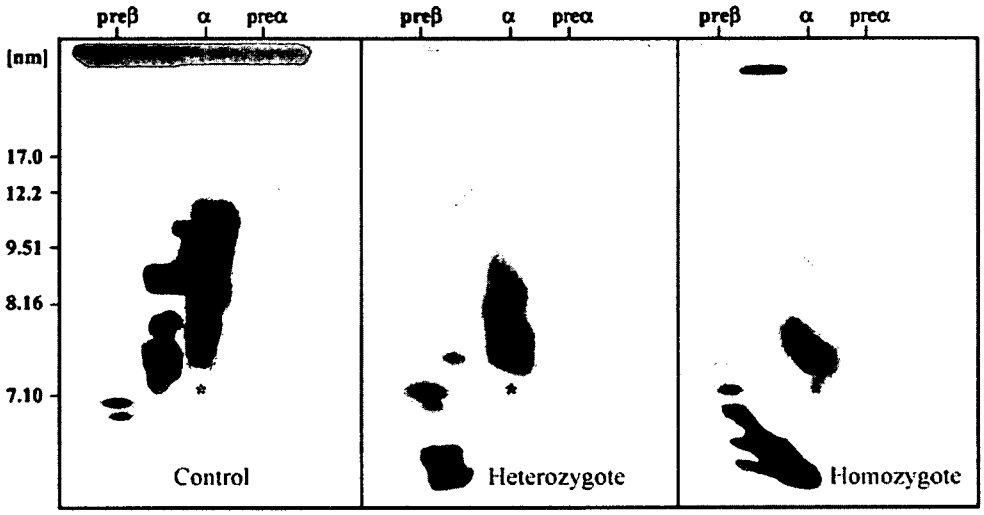

Fig. 5. ApoC-III-containing HDL subpopulations of representative control, heterozygous, and homozygous LCAT-deficient subjects superimposed on the image of apoA-I-containing subpopulations. In controls, the majority of apoC-III comigrates with apoA-I in α-1 and α-2 HDL, and some has also been found in the α-3 and α-4 size range with no comigration with apoA-I. In homozygotes and heterozygotes, practically all apoC-III has been detected in small, lipid-poor HDL particles. The asterisk represents the endogenous human serum albumin marking the α-mobility front.

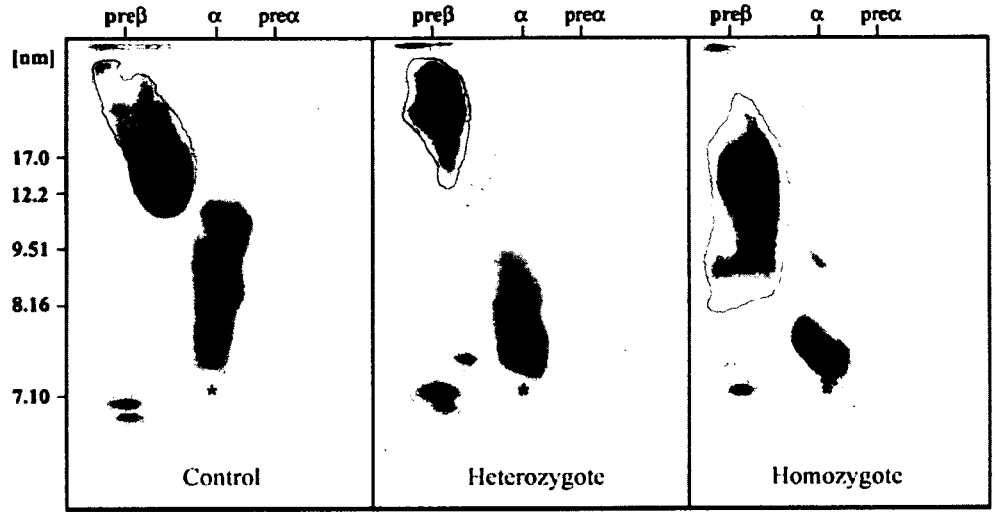

Fig. 6. ApoE-containing HDL subpopulations of representative control, heterozygous, and homozygous LCAT-deficient subjects superimposed on the image of apoA-I-containing subpopulations. There is no comigration of apoE- and apoA-I-containing particles. The asterisk represents the endogenous human serum albumin marking the α-mobility front.

necessary for the transformation of preβ-1 HDL into α-mobility HDL. Preβ-1 binds to ABCA1 and removes phospholipids and unesterified cholesterol from cells (13). During this process, there are probably changes in apoA-I conformation and electrophoretic charge. We hypothesize that α-4 HDL contains two molecules of apoA-I, as is the case for preβ-1 HDL. Larger (~8 nm–20 nm) α-mobility HDL particles have also been observed in many of the homozygotes. The tight bands of these particles suggest that these are poorly lipidated, discoidal HDL aggregates. We have no data indicating whether LCAT can act on these large, stacked disks or can use only the small α-4 HDL as a substrate. The apoA-I-containing HDL subpopulation profile of heterozygotes resembles that of low HDL-C CAD patients, inasmuch as apoA-I distribution is shifted toward the smaller particles. ApoA-II is dramatically reduced in homozygous subjects, probably because of fast catabolism (18), and, interestingly, it comigrates with preβ-1 HDLs, which normally contain only apoA-I. Some apoA-II also comigrates with preβ-1 HDL in heterozygotes; however, we do not know whether apoA-I and apoA-II are in the same particles. As a result of the presence of cholesteryl ester in the core of HDL particles, apoA-II binds to α-2 and α-3 HDL particles very early, as indicated in heterozygotes whose apoA-I/apoA-II ratios are increased in these particles. Our data also suggest that LCAT is not a key player in the formation of apoA-IV-containing particles. On the basis of these and other findings (16, 17), we hypothesize that the metabolism of apoA-IV-containing particles is independent of ABCA-1-mediated cellular cholesterol efflux, as well as of CETP and LCAT activities in humans. The majority of apoC-I comigrates with apoA-I-containing α-1 HDL in controls. About 20% of apoC-I in controls and ~35% of apoC-I in heterozygotes have α-mobility with larger than α-1 size. Homozygotes have apoC-I only in the VLDL fraction, indicating that the neutral lipid core is essential for the incorporation of apoC-I into HDL. ApoC-III has a complex pattern in controls: ~25% of apoC-III comigrates with α-1, ~50% comigrates with α-2, ~15% is found in VLDL, and the rest is in the HDL size range but does not overlap with apoA-I-containing particles. Interestingly, in both affected groups, apoC-III has been detected in small, lipid-poor form (free apoC-III), indicating that apoC-III is probably sensitive to the lipid and apolipoprotein composition of HDL. The large amount of free apoC-III in affected subjects also indicates that the fractional catabolic rate of this apolipoprotein is not increased with decreased particle size, which is clearly not the case for apoA-I and apoA-II. We clearly demonstrate that apoE-containing particles do not overlap with apoA-I-containing particles either in controls or in LCAT-deficient subjects in this study. [We have only seen apoE comigrating with apoA-I in homozygous CETP-deficient subjects where HDL size reached the size of LDL and the particles were probably loaded with excess amounts of cholesteryl ester (17)]. Although apoA-I concentrations were significantly lower in the large particles in heterozygous LCAT-deficient subjects, apoE concentrations were significantly increased in the large apoE HDL particles in these subjects. We have no explanation for this phenomenon. We do not know the chemical composition of these particles. In homozygous LCAT-deficient subjects, we observed only slightly more apoE in apparently lipid-poor particles. Therefore, LCAT activity does not seem to be a key player in supplying neutral lipids for apoE-containing HDL. Alternatively, TGs seem to be sufficient for the formation of the core of apoE HDL in homozygotes. If this is true, the questions arise as to how this TG-rich apoE HDL is metabolized and what its role in lipoprotein metabolism and CAD risk is.

Our current concept of HDL remodeling in vivo in humans, presented in **Fig. 7**, is based on data generated in various genetic states associated with alterations in HDL metabolism (ABCA1, LCAT, and CETP deficiency). We are in the process of examining HDL subpopulations in other genetic disorders as well [apoA-I deficiency, apoE deficiency, abetalipoproteinemia, lipoprotein lipase (LPL) deficiency, and hepatic lipase (HL) deficiency]. On the basis of our observations, we describe the following steps in HDL metabolism.

Step 1: synthesis

ApoA-I is synthesized in the liver and small intestine, and two molecules of apoA-I form a belted structure around ~16 molecules of phospholipids to form discoidal preβ-1 HDL in the interstitial or plasma compartment.

Step 2: cellular cholesterol efflux

Preβ-1 particles pick up FC and more phospholipids from cells via the ABCA1 pathway and are transformed into small, lipid-poor, discoidal LpA-I α-4 HDL particles.

Step 3: cholesterol esterification

LCAT esterifies FC on the surface of HDL into cholesteryl esters, which move into the core with an increase in HDL particle size.

Step 4: TG hydrolysis

LPL hydrolyzes TGs in TG-rich lipoprotein (TRL), resulting in surface components (phospholipids, FC, and apolipoproteins) available and necessary for HDL particle size increase.

The concerted actions of ABCA1, LCAT, and LPL continuously increase HDL particle size (steps 2–4).

Step 5: cholesteryl ester exchange (CETP cycle)

With CETP-mediated exchange of core cholesteryl esters for TG between large HDL particles and TRL, differentiated α- and preα-migrating HDL particles form; these contain apoA-I with apoA-II, or apoA-I without apoA-II, or apoE only. CETP can also exchange cholesteryl esters for TG among HDL particles and, as a result, a substantial amount of preβ-1 forms.

Step 6: phospholipid hydrolysis

HL, endothelial lipase (EL), and secretory phospholipase A2 (sPLA2) hydrolyze TG and phospholipids on HDL, resulting in size reduction of large α-1 into α-2 HDL (HL), or disintegration of all larger HDL particles into α-4 and preβ-1 (EL), or preβ-1 and free apoA-I (sPLA2).

Step 7: hepatic cholesteryl ester uptake (SR-BI cycle)

Cholesteryl esters on α-2 and α-1 HDL particles are selectively transported from HDL particles to the liver via SR-BI for ultimate excretion of cholesterol into the bile, resulting in recycling of apolipoproteins, phospholipids, and FC from these larger HDL particles to small α-4 HDL.

The concerted actions of CETP, SR-BI, and lipases decrease HDL particle size (steps 5–7).

Step 8: apolipoprotein catabolism

Clearance of small, lipid-poor apoA-I particles: the final step in HDL particle metabolism is the uptake of whole HDL particles by the liver and cubulin/megalin-mediated clearance of free apoA-I and preβ-1 HDL in the kidney.

Based on the observations presented here, our data are consistent with the concept that LCAT plays a crucial role in the maturation of HDL particles (steps 2–4).

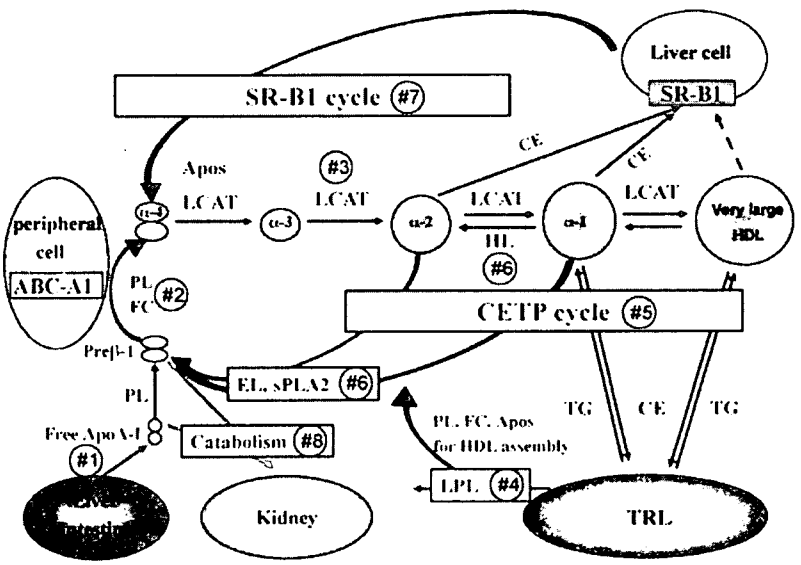

Fig. 7. Current concept of HDL remodeling in humans in vivo. Abbreviations not used in the text: phospholipids (PL), cholesteryl ester (CE).

This study was supported by Grant HL-64738 from the National Institutes of Health/National Heart, Lung, and Blood Institute (B.F.A.), USDA Grant 53-1950-5-003 (E.J.S.), Telethon-Italy Grant GGP02264 (L.C.), Fondazione Cariplo Grant 2003-1753 (G.F.), and Grant PRIN2005 from the Italian Ministry of University (L.C., G.F.). The authors are indebted to Drs. M. Arca, S. Bertolini, G. Bittolo Bon, G. Boscutti, G. Busnach, G. Frascà, L. Gesualdo, G. Lupattelli, I. Rabbone, G. Ruotolo, T. Sampietro, and A. Sessa for the identification of the Italian LCAT-deficient families.

REFERENCES

1. McLean, J., C. Fielding, D. Drayna, H. Dieplinger, B. Baer, W. Kohr, W. Henzel, and R. Lawn. 1986. Cloning and expression of human lecithin-cholesterol acyltransferase cDNA. *Proc. Natl. Acad. Sci. USA.* **83:** 2335–2339.
2. Fielding, C. J., and P. E. Fielding. 1995. Molecular physiology of reverse cholesterol transport. *J. Lipid Res.* **36:** 211–228.
3. Czarnecka, H., and S. Yokoyama. 1996. Regulation of cellular cholesterol efflux by lecithin:cholesterol acyltransferase reaction through nonspecific lipid exchange. *J. Biol. Chem.* **266:** 2023–2028.
4. Jonas, A., A. von Eckardstein, K. E. Kezdy, A. Steinmetz, and G. Assmann. 1991. Structural and functional properties of reconstituted high density lipoprotein discs prepared with six apolipoprotein A-I variants. *J. Lipid Res.* **32:** 97–106.
5. Steinmetz, A., H. Kaffarnik, and G. Utermann. 1985. Activation of phosphatidylcholine-sterol acyltransferase by human apolipoprotein E isoforms. *Eur. J. Biochem.* **152:** 747–751.
6. Kuivenhoven, J. A., H. Pritchard, J. Hill, J. Frohlich, G. Assmann, and J. Kastelein. 1997. The molecular pathology of lecithin:cholesterol acyltransferase (LCAT) deficiency syndromes. *J. Lipid Res.* **38:** 191–205.
7. Santamarina-Fojo, S., J. M. Hoeg, G. Assmann, and H. B. Brewer, Jr. 2001. Lecithin cholesterol acyltransferase deficiency and fish eye disease. *In* The Metabolic and Molecular Bases of Inherited Disease. C. R. Scriver, A. L. Beaudet, W. S. Sly, D. Valle, editors. McGraw-Hill, New York. 2817–2834.
8. Gordon, D. J., and B. M. Rifkind. 1989. High-density lipoprotein—the clinical implications of recent studies. *N. Engl. J. Med.* **321:** 1311–1316.
9. Funke, H., A. von Eckardstein, P. H. Pritchard, J. J. Albers, J. J. Kastelein, C. Droste, and G. Assmann. 1991. A molecular defect causing fish eye disease: an amino acid exchange in lecithin-cholesterol acyltransferase (LCAT) leads to the selective loss of alpha-LCAT activity. *Proc. Natl. Acad. Sci. USA.* **88:** 4855–4859.
10. Brousseau, M. E., S. Santamarina-Fojo, B. L. Vaisman, D. Applebaum-Bowden, A. M. Berard, G. D. Talley, H. B. Brewer, Jr., and J. M. Hoeg. 1997. Overexpression of human lecithin:cholesterol acyltransferase in cholesterol-fed rabbits: LDL metabolism and HDL metabolism are affected in a gene dose-dependent manner. *J. Lipid Res.* **38:** 2537–2547.
11. Berard, A. M., B. Foger, A. Remaley, R. Shamburek, B. L. Vaisman, G. Talley, B. Paigen, R. F. Hoyt, Jr., S. Marcovina, H. B. Brewer, Jr., et al. 1997. High plasma HDL concentrations associated with enhanced atherosclerosis in transgenic mice overexpressing lecithin-cholesteryl acyltransferase. *Nat. Med.* **3:** 744–749.
12. Foger, B., M. Chase, M. J. Amar, B. L. Vaisman, R. D. Shamburek, B. Paigen, J. Fruchart-Najib, J. A. Paiz, C. A. Koch, R. F. Hoyt, et al. 1999. Cholesteryl ester transfer protein corrects dysfunctional high density lipoproteins and reduces aortic atherosclerosis in lecithin cholesterol acyltransferase transgenic mice. *J. Biol. Chem.* **274:** 36912–36920.
13. Asztalos, B. F., M. de la Llera-Moya, G. E. Dallal, K. V. Horvath, E. J. Schaefer, and G. H. Rothblat. 2005. Differential effects of HDL subpopulations on cellular ABCA1- and SR-BI-mediated cholesterol efflux. *J. Lipid Res.* **46:** 2246–2253.
14. Calabresi, L., L. Pisciotta, A. Costantin, I. Frigerio, I. Eberini, P. Alessandrini, M. Arca, G. B. Bon, G. Boscutti, G. Busnach, et al. 2005. The molecular basis of lecithin:cholesterol acyltransferase deficiency syndromes: a comprehensive study of molecular and biochemical findings in 13 unrelated Italian families. *Arterioscler. Thromb. Vasc. Biol.* **25:** 1972–1978.
15. Asztalos, B. F., M. Lefevre, T. A. Foster, R. Tulley, M. Windhauser, L. Wong, and P. S. Roheim. 1997. Normolipidemic subjects with low HDL cholesterol levels have altered HDL subpopulations. *Arterioscler. Thromb. Vasc. Biol.* **17:** 1885–1893.
16. Asztalos, B. F., M. E. Brousseau, J. R. McNamara, K. V. Horvath, P. S. Roheim, and E. J. Schaefer. 2001. Subpopulations of high density lipoproteins in homozygous and heterozygous Tangier disease. *Atherosclerosis.* **156:** 217–225.
17. Asztalos, B. F., K. V. Horvath, K. Kajinami, C. Nartsupha, C. E. Cox, M. Batista, E. J. Schaefer, A. Inazu, and H. Mabuchi. 2004. Apolipoprotein composition of HDL in cholesteryl ester transfer protein deficiency. *J. Lipid Res.* **45:** 448–455.
18. Rader, D. J., K. Ikewaki, N. Duverger, H. Schmidt, H. Pritchard, J. Frohlich, M. Clerc, M. F. Dumon, T. Fairwell, L. Zech, et al. 1994. Markedly accelerated catabolism of apolipoprotein A-II (apoA-II) and high density lipoproteins containing apoA-II in classic lecithin:cholesterol acyltransferase deficiency and fish-eye disease. *J. Clin. Invest.* **93:** 321–330.

JOURNAL OF LIPID RESEARCH

Increased lipid rafts and accelerated lipopolysaccharide-induced tumor necrosis factor-α secretion in Abca1-deficient macrophages[S]

Masahiro Koseki,[1,*] Ken-ichi Hirano,[*,†] Daisaku Masuda,[*] Chiaki Ikegami,[*] Masaki Tanaka,[§] Akemi Ota,[*] Jose C. Sandoval,[†] Yumiko Nakagawa-Toyama,[*] Satoshi B. Sato,[**] Toshihide Kobayashi,[††] Yukiko Shimada,[§§] Yoshiko Ohno-Iwashita,[§§] Fumihiko Matsuura,[*,†] Iichiro Shimomura,[*] and Shizuya Yamashita[*,†]

Department of Metabolic Medicine,* Cardiovascular Medicine,† and Medicine and Pathology,§ Graduate School of Medicine, Osaka University, Suita, Osaka, Japan; Department of Biophysics,** Graduate School of Science, Kyoto University, Kyoto, Japan; RIKEN,†† Wako, Saitama, Japan; and Biomembrane Research Group,§§ Tokyo Metropolitan Institute of Gerontology, Itabashi-ku, Tokyo, Japan

Abstract **Lipid rafts on the cell surface are believed to be very important as platforms for various cellular functions. The aim of this study was to know whether defective lipid efflux may influence lipid rafts on the cell surface and their related cellular functions. We investigated macrophages with defective lipid efflux from ATP binding cassette transporter A1-deficient (Abca1-KO) mice. Lipid rafts were evaluated by the following two novel probes: a biotinylated and protease (subtilisin Carlsberg)-nicked derivative of θ-toxin and a fluorescein ester of polyethylene glycol-derived cholesterol. Lipid rafts in Abca1-KO macrophages were increased, as demonstrated by both probes. Moreover, activities of nuclear factor κB, mRNA and intracellular distribution, and secretion of tumor necrosis factor-α (TNF-α) were examined after stimulation by lipopolysaccharides (LPSs). LPS-induced responses of the activation of nuclear factor κB and TNF-α were more prompt and accelerated in the Abca1-KO macrophages compared with wild-type macrophages. Modification of lipid rafts by cyclodextrin and nystatin corrected the abnormal response, suggesting an association between the increased lipid rafts and abnormal TNF-α secretion.[S] We report here that Abca1-KO macrophages with defective lipid efflux exhibited increased lipid rafts on the cell surface and accelerated TNF-α secretion.**—Koseki, M., K-i. Hirano, D. Masuda, C. Ikegami, M. Tanaka, A. Ota, J. C. Sandoval, Y. Nakagawa-Toyama, S. B. Sato, T. Kobayashi, Y. Shimada, Y. Ohno-Iwashita, F. Matsuura, I. Shimomura, and S. Yamashita. **Increased lipid rafts and accelerated lipopolysaccharide-induced tumor necrosis factor-α secretion in Abca1-deficient macrophages.** *J. Lipid Res.* **2007.** 48: **299–306.**

Supplementary key words ATP binding cassette transporter A1 • biotinylated and protease (subtilisin Carlsberg)-nicked derivative of θ-toxin • cholesterol efflux • lipid rafts • polyethylene glycol-derived cholesterol • tumor necrosis factor-α

Manuscript received 27 September 2006 and in revised form 31 October 2006.

Published, JLR Papers in Press, November 7, 2006.
DOI 10.1194/jlr.M600428-JLR200

Reverse cholesterol transport (RCT) is one of the major protective systems against atherosclerosis, in which HDL particles play a crucial role as a shuttle carrying cholesterol derived from peripheral tissues to the liver (1). Cholesterol efflux from the cells is the initial step of RCT, in which free apolipoprotein A-I (apoA-I) or small HDLs take up cholesterol from the peripheral cells. We have been trying to elucidate the molecular mechanism for RCT and cholesterol efflux by analyzing the pathophysiology of patients with abnormal HDL metabolism. We have identified molecules involved in cellular cholesterol efflux and apoA-I and HDL binding proteins on macrophages (2–5).

Tangier disease (TD) is a model for the impairment of cholesterol efflux from the cells (6, 7). Patients with TD suffer from genetic HDL deficiency, hepatosplenomegaly, orange tonsils, and premature atherosclerosis (8, 9). Many laboratories including ours have reported that mutations in the Abca1 gene lead to defective cholesterol efflux from the cells (10–12). As a result of the mutation(s) in the Abca1 gene, cells from TD patients exhibited a deficiency of apoA-I-mediated cholesterol efflux and a subsequent accumulation of intracellular lipids as lipid droplets, which is closely related to the development of atherosclerosis in this disorder.

On the other hand, in the plasma membrane, cholesterol is distributed abundantly in some domain structures

Abbreviations: Abca1-KO, ATP binding cassette transporter A1-deficient; apoA-I, apolipoprotein A-I; BCθ, biotinylated and protease (subtilisin Carlsberg)-nicked derivative of θ-toxin; fPEG-chol, fluorescent polyethylene glycol cholesteryl ether; LPS, lipopolysaccharide; NF-κB, nuclear factor-κB; 2OHpβCD, 2-hydroxypropyl-β-cyclodextrin; RCT, reverse cholesterol transport; TD, Tangier disease; TNF-α, tumor necrosis factor-α; WT, wild-type.

[1] To whom correspondence should be addressed.
e-mail: koseki@imed2.med.osaka-u.ac.jp

[S] The online version of this article (available at http://www.jlr.org) contains supplementary data in the form of figures.

called "lipid rafts," "cholesterol-rich microdomains," or "detergent-resistant membranes" (13). These domains are enriched in cholesterol and sphingolipids and contain specific proteins, including glycosylphosphatidylinositol-anchored proteins, and are believed to be important as rafts mediating some intracellular and/or extracellular signals (14–20). Recently, the following two probes were developed to visualize rafts. One is a biotinylated and protease (subtilisin Carlsberg)-nicked derivative of θ-toxin (BCθ) (21–25). This probe was developed by Ohno-Iwashita et al. (21–25) and is derived from a thiol-activated cytolysin produced by *Clostridium perfringens*. BCθ selectively binds to membrane cholesterol in lipid rafts. The other probe is a polyethylene glycol cholesteryl ether (26, 27). This compound belongs to a unique group of nonionic amphipathic cholesterol derivatives. It can bind with cholesterol-rich membranes both in cells and in model membranes. It was recently reported that a fluorescent polyethylene glycol cholesteryl ether (fPEG-chol) is a sensitive probe for unraveling the dynamics of cholesterol-rich microdomains in living cells.

Little is known about the effect of defective lipid efflux on lipid rafts in plasma membranes. In this study, we have tested the hypothesis that defective efflux influences lipid rafts in the plasma membrane and examined related cellular functions using ATP binding cassette transporter A1-deficient (Abca1-KO) macrophages as a model.

METHODS

Materials

BCθ and fPEG-chol were prepared as described previously (26, 28).

Animal treatment and cell culture

Abca1-KO mice created on the DBA1 lac/J background (29) were purchased from the Jackson Laboratory. Mice were fed a normal chow diet. The experimental protocol was approved by the Ethics Review Committee for Animal Experimentation of Osaka University Graduate School of Medicine. After an intraperitoneal injection of 2 ml of 4% thioglycollate (B-2551; Sigma-Aldrich) medium, mouse peritoneal macrophages were harvested from Abca1-KO and wild-type (WT) mice. The cells were cultured according to standard conditions in Dulbecco's minimum essential medium supplemented with L-glutamine, nonessential amino acids, and 10% fetal calf serum in a humidified 5% CO_2 atmosphere at 37°C. Human monocyte-derived macrophages from a TD patient and healthy volunteers were prepared after informed consent was obtained. ABCA1-null fibroblasts were obtained from two unrelated male patients with TD after informed consent was obtained.

Fluorescence labeling for confocal laser microscopy

The cells were washed with ice-cold PBS and treated with 10 μg/ml BCθ for 30 min on ice. After rinsing, the cells were fixed with 4% formaldehyde and incubated with streptavidin-Alexa Flour 594 conjugate for 30 min (S-11227; Molecular Probes). The nuclei were stained with 4′,6-diamino-phenylindole. In other experiments for fPEG-chol, cells were fixed and treated with 0.2% gelatin for 30 min and then incubated with 1 μg/ml fPEG-chol for 5 min at room temperature. Images were acquired for each fluorescent probe by confocal laser microscopy (LSM510; Carl Zeiss).

Fractionation by sucrose density gradient ultracentrifugation

After incubation with 10 μg/ml BCθ for 30 min on ice, mouse peritoneal macrophages were harvested and sucrose gradient ultracentrifugation was performed as described previously (25). Free cholesterol levels were measured using the Amplex Red cholesterol assay method (Molecular Probes) (25).

Detection of BCθ bound to cells by Western blot analysis

The lysates of BCθ-bound cells were subjected to SDS-PAGE, and Western blot analysis was performed as described previously (25).

Construction of adenovirus vectors and their expression in fibroblasts

FLAG-tagged human Abca1 cDNA with the FLAG epitope (DYKDDDDK) incorporated at its C terminus (hAbca1/FLAG) was generated by PCR. Adenovirus vectors encoding LacZ and hAbca1/FLAG were constructed according to the protocol of the Adeno X expression system (Clontech). Infection with adenovirus was carried out by incubating cells in serum-free medium for 1 h at 37 °C under gentle agitation. After incubation, complete medium was supplied, and the cells were further incubated in a CO_2 incubator. Five days after infection with the indicated multiplicity of infection, the cells were used in the experiments.

Measurement of tumor necrosis factor-α levels and nuclear factor-κB p65 activities

The mouse peritoneal macrophages were plated on 24-well plates and incubated with 10 ng/ml lipopolysaccharide (LPS) of *Escherichia coli* strain O55:B5 (L-6529; Sigma-Aldrich). The amount of tumor necrosis factor-α (TNF-α) in the culture medium was determined by ELISA (mouse TNF-α ELISA kit; Biosource). Nucleoproteins were extracted from the macrophages (Nuclear Extract Kit; Active Motif), and nuclear factor-κB (NF-κB) p65 activity was measured according to the manufacturer's protocols (TransAM NF-κB p65 Chemi; Active Motif).

RNA isolation, cDNA synthesis, and quantitative PCR

Total RNA was isolated from mouse macrophages using the RNeasy Mini Kit (Qiagen), followed by treatment with DNase I (Qiagen). Of each RNA sample, 1 μg of total RNA was primed with 50 pmol of oligo(dT)20 and reverse-transcribed with SuperScript III RT (200 units; Invitrogen), according to the protocol of the manufacturer. Real-time quantitative PCR was performed according to the protocol of the DyNAmo HS SYBR Green quantitative PCR kit. To assess the expression levels of TNF-α mRNA in macrophages, DNA polymerase and SYBR Green I were used in a reaction volume of 20 μl using gene-specific primers (5 mM) on cDNA (corresponding to ~50 ng of total RNA) (8, 30).

Primers used in this study

Each set of primers located different exons: primer 1, 5′-ccagaccctcacactcagatca-3′, mouse TNF-α cDNA, nucleotides 381–402 (GenBank accession number NM_013693); primer 2, 5′-cacttggtggtttgctacgac-3′, mouse TNF-α cDNA, nucleotides 459–439 (GenBank accession number NM_013693); primer 3, 5′-ggagccaaacgggtcatcatctc-3′, mouse GAPDH cDNA, nucleotides 383–405 (GenBank accession number M32599); primer

4, 5′-gaggggccatccacagtcttct-3′, mouse GAPDH cDNA, nucleotides 615–594 (GenBank accession number M32599).

RESULTS

Lipid rafts were increased in Abca1-KO macrophages

Lipid rafts on the plasma membrane were visualized using two different probes, BCθ and fPEG-chol. Confocal laser scanning microscopy revealed that both probes recognized a greater volume of lipid rafts in the mouse peritoneal macrophages from Abca1-KO mice than from WT mice (**Fig. 1A**). Similar results were obtained in human monocyte-derived macrophages from a TD patient (9) and from normal subjects (Fig. 1B). These results suggested that lipid rafts on the plasma membrane were increased in Abca1-KO macrophages. As the number of the patient macrophages was limited, we made use of mouse macrophages in the experiments described below.

To confirm whether BCθ recognizes cholesterol-rich domains in mouse peritoneal macrophages, sucrose density gradient ultracentrifugation was performed. In both Abca1-KO and WT macrophages, the distribution of free cholesterol concentration consisted of two peaks: low density raft fractions (fractions 2–5) and high density nonraft fractions (fractions 8–10) (**Fig. 2A**). The sums of cholesterol content in the raft fractions (fractions 2–5) and in the nonraft fractions (fractions 8–10) were calculated, showing that the free cholesterol content of lipid rafts was increased significantly in Abca1-KO macrophages and that the free cholesterol content of nonrafts was not significantly different between WT and Abca1-KO macrophages (Fig. 2B). As expected, BCθ was distributed mainly in low-density, Triton X-100-insoluble membrane fractions (fractions 2–5), as shown by Western blot analysis, in both Abca1-KO and WT macrophages, and BCθ binding to rafts of Abca1-KO macrophages was detected more strongly than to rafts of WT macrophages (Fig. 2A).

Abca1 complementation corrected abnormal lipid rafts

Furthermore, to analyze the relationship between Abca1 and lipid rafts, we performed a complementary experiment using TD fibroblasts. The lipid rafts in TD fibroblasts were increased (see supplementary Fig. 1A). We generated the adenovirus encoding human Abca1 and examined its effect on binding of BCθ to TD fibroblasts. Confocal laser scanning microscopy and Western blot analysis clearly showed a multiplicity of infection-dependent decrease in BCθ binding (see supplementary Fig. 1B). This result indicated that introduction of the Abca1 gene corrected the phenotype of TD fibroblasts, suggesting a causal relationship between Abca1 deficiency and the alteration of lipid rafts.

Abnormal cytokine secretion from Abca1-KO macrophages

We supposed that the increase of lipid rafts, as well as intracellular lipid storage, might affect the process of premature atherosclerosis in patients with TD. We hypothesized that the increase of lipid rafts might affect the activation of nuclear receptors and the subsequent synthesis and secretion of cytokines in macrophages, because some papers reported that lipid rafts might play a pivotal role in the cellular recognition of LPS (31). Therefore, we focused on LPS-induced intracellular signaling and cytokine secretion, particularly at an acute phase after

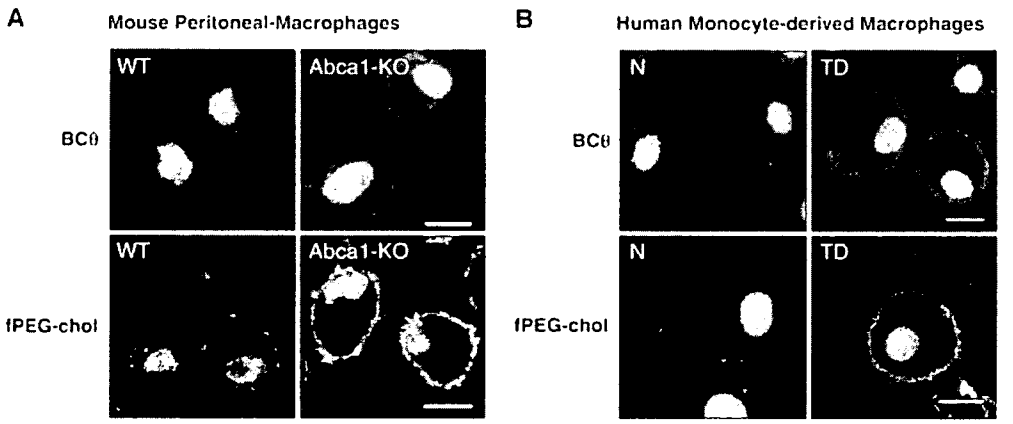

Fig. 1. Visualized lipid rafts in mouse and human macrophages. A: ATP binding cassette transporter A1-deficient (Abca1-KO) and wild-type (WT) mouse peritoneal macrophages were washed once with ice-cold PBS and treated with 10 μg/ml biotinylated and protease (subtilisin Carlsberg)-nicked derivative of θ-toxin (BCθ) for 30 min on ice. After rinsing, the cells were fixed with 4% formaldehyde and incubated with streptavidin-Alexa Flour 594 conjugate (S-11227; Molecular Probes) for 30 min (red). The nuclei were stained with 4′,6-diamino-phenylindole (blue). In the experiments for fluorescent polyethylene glycol cholesteryl ether (fPEG-chol), macrophages were fixed and treated with 0.2% gelatin for 30 min, then incubated with 0.5 μg/ml fPEG-chol for 5 min (green). Images were acquired for each fluorescent probe by confocal laser microscopy (LSM510; Carl Zeiss). The results shown are representative of three independent experiments. Bars = 10 μm. B: Human monocyte-derived macrophages from a Tangier disease (TD) patient and a normal subject (N) were also examined. The results shown are a representative of three independent experiments. Bars = 10 μm.

JOURNAL OF LIPID RESEARCH

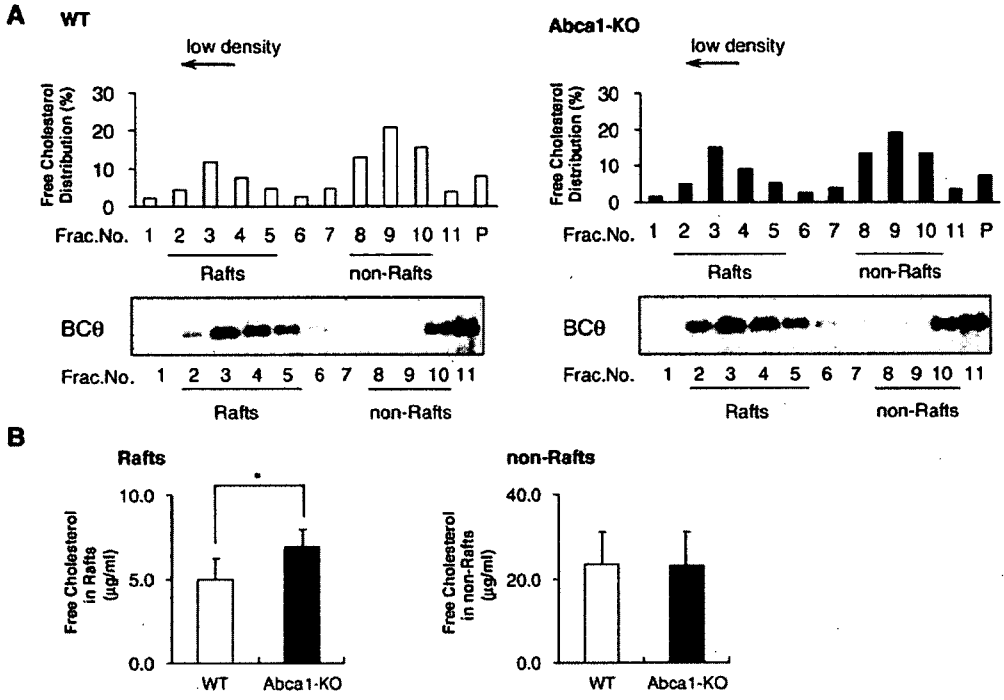

Fig. 2. Sucrose gradient fractionation confirmed that BCθ recognized lipid rafts in mouse peritoneal macrophages. A: BCθ-treated mouse macrophages were incubated with 1% Triton X-100 at 4°C for 30 min. Equal amounts of protein homogenates were subjected to sucrose gradient ultracentrifugation and fractionated from the top [fractions 1–11 and pellet (P); the pellet was suspended and sonicated in buffered saline], as described in Methods. To determine the distribution of free cholesterol and BCθ, the same volume of each fraction was subjected to the quantification of cholesterol and Western blot analysis. BCθ binding to lipid rafts in Abca1-KO and WT macrophages was selectively detected in Triton X-100-insoluble raft fractions by Western blot analysis. The amount of BCθ binding to lipid rafts in Abca1-KO macrophages was greater than that in WT macrophages. The signals of BCθ in the bottom fraction 11 seemed to be free BCθ. The results shown are representative of three independent experiments. B: The sums of cholesterol contents in lipid raft fractions (fractions 2–5) and in nonlipid raft fractions (fractions 8–10) were compared between Abca1-KO and WT macrophages. Free cholesterol contents were significantly higher in lipid rafts of Abca1-KO macrophages than in those of WT macrophages. Values shown are mean ± SEM. * $P < 0.05$ by Student's *t*-test.

LPS stimulation. As shown in **Fig. 3A**, activities of NF-κB p65 were induced only at 15 min in both Abca1-KO and WT macrophages, and the activity was significantly higher in Abca1-KO macrophages than in WT macrophages throughout the time course. Figure 3B shows the TNF-α mRNA levels. TNF-α mRNA levels were induced at 30 min and reached a peak at 45 min in both Abca1-KO and WT macrophages. TNF-α mRNA in Abca1-KO macrophages was significantly higher than in WT macrophages at any time point after 30 min. Figure 3C demonstrates the immunocytochemical analysis for TNF-α (32). Before LPS stimulation, we could not detect the immunoreactive mass of TNF-α in either macrophages. After 1 h, the immunoreactive mass of TNF-α was detected in perinuclear organelles in Abca1-KO macrophages but not in WT macrophages. After 2 h, the immunoreactive mass of TNF-α was found more dispersed in the cytoplasm of Abca1-KO macrophages. Figure 3D shows TNF-α secretion data. A significant difference in TNF-α secretion into the medium occurred at 1 h after LPS stimulation. Similarly, the secretion of interleukin-6 into the medium was significantly higher in Abca1-KO macrophages than in WT macrophages (see supplementary Fig. II). These data suggest that an acute phase response to LPS seems to be accelerated in Abca1-KO macrophages.

Effect of lipid raft modulators on mRNA and release of TNF-α

Finally, we investigated the relationship between increased lipid rafts and the accelerated response of TNF-α in Abca1-KO macrophages. We used the following two lipid raft modulators: 2-hydroxypropyl-β-cyclodextrin (2OHpβCD) and nystatin (21, 31, 33). **Figure 4A** shows the effect of 2OHpβCD, which selectively depleted cholesterol from lipid rafts, on staining with BCθ. The signals of BCθ were diminished after 2OHpβCD treatment in both macrophages. Figure 4B indicates the effect of the depletion of rafts on TNF-α mRNA levels and TNF-α secretion from macrophages. After treatment with 20 mM 2OHpβCD, the LPS-induced expression of TNF-α was decreased significantly in Abca1-KO and WT macrophages. The depletion of cholesterol from rafts by treatment with 20 mM 2OHpβCD diminished the significant difference in TNF-α mRNA levels and TNF-α secretion between Abca1-

JOURNAL OF LIPID RESEARCH ASBMB

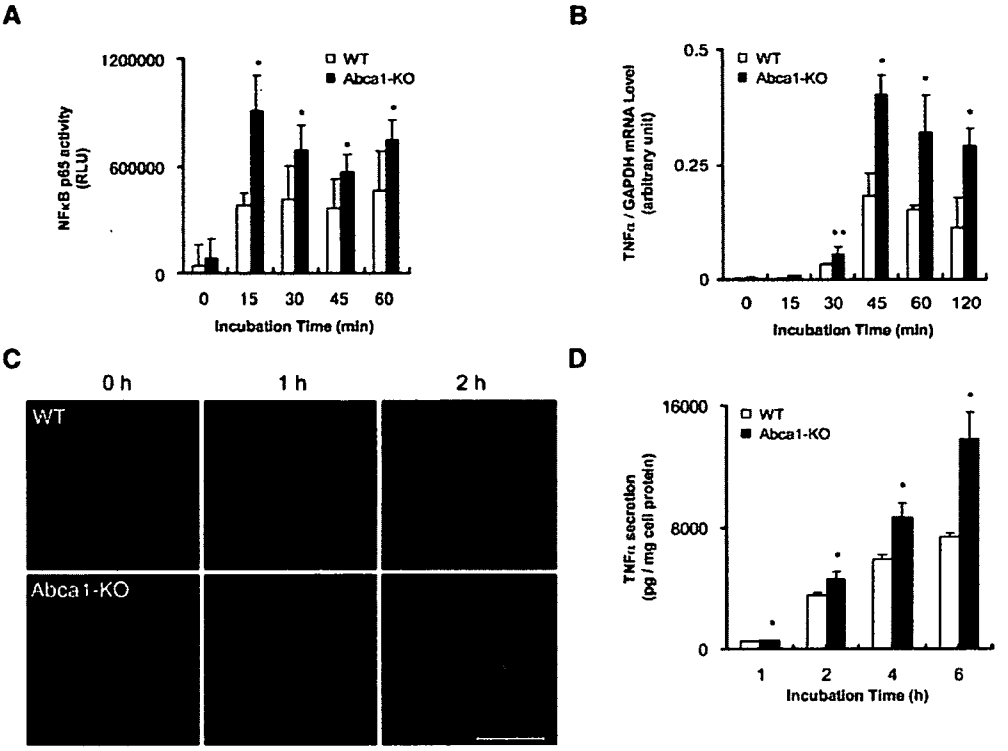

Fig. 3. Activities of nuclear factor-κB (NF-κB) and mRNA and release of tumor necrosis factor-α (TNF-α) from Abca1-KO macrophages. The 1.5×10^6 peritoneal macrophages of Abca1-KO or WT mice were seeded on 24-well plates. After 2 days, the macrophages were incubated with 10 ng/ml lipopolysaccharide (LPS) of *Escherichia coli* strain O55:B5 (L-6529; Sigma-Aldrich) for the indicated time in each experiment. A: Nucleoprotein was extracted from the macrophages (Nuclear Extract Kit; Active Motif), and NF-κB p65 activity was measured (TransAM NF-κB p65 Chemi; Active Motif). B: Total RNA was isolated from the macrophages, and TNF-α mRNA levels were evaluated by real-time quantitative PCR. C: The macrophages were fixed and stained with goat anti-TNF-α antibody (Molecular Probes) and goat anti-Alexa Flour 488. The nuclei were stained with 4′,6-diamino-phenylindole. Images were acquired by confocal laser microscopy (LSM510; Carl Zeiss). Bar = 20 μm. D: TNF-α in the medium was measured by ELISA (mouse TNF-α ELISA kit; Biosource). Means and SD values were calculated from the data from three independent experiments. * $P < 0.05$, ** $P < 0.01$ by Student's *t*-test.

KO and WT macrophages. Next, as shown in Fig. 4C, we tested another lipid raft modulator, nystatin, which was shown to disrupt cholesterol-rich domains. After treatment with nystatin, the expression of TNF-α was also decreased significantly in both macrophages. Treatment with 25 μg/ml nystatin attenuated the significant difference of TNF-α mRNA levels between Abca1-KO and WT macrophages. These data strongly suggested that Abca1-KO macrophages were more affected by lipid raft modulators because of the increase of lipid rafts. The alteration of lipid rafts may regulate the acute response of TNF-α by LPS stimulation.

DISCUSSION

Lipid rafts and atherosclerosis

Lipid bilayers in the plasma membrane were previously believed to be homogeneous. Recently, a number of studies revealed that lipid rafts could play an essential role in many cellular processes, including signal transduction, membrane trafficking, cytoskeletal organization, and many other cellular events (17–20, 34, 35). Even though many studies focused on the distribution pattern of membrane proteins in lipid rafts, there is little evidence that a particular genetic defect might affect the number of lipid rafts and subsequent cellular functions. One reason for this might be the complexity and difficulty of measuring lipid rafts. In this study, we have succeeded relatively easily in comparing the volume of lipid rafts using two newly developed lipid raft probes. Here, for the first time, we report that a mutation in a single gene might alter lipid rafts and that the increase in lipid rafts might be related to the acceleration of atherogenic processes. In this study, we focused on the acute secretion to LPS stimulation. Recently, Ishiwata et al. (26) and Kay et al. (36) reported on the importance of cholesterol-rich lipid rafts in the delivery of TNF-α to the plasma membrane and the exit sites for cytokine secretion. It would be of interest to investigate whether the increased lipid rafts in the Abca1-KO macrophages might affect the exocytosis of cytokines. Further studies will be necessary to clarify this.

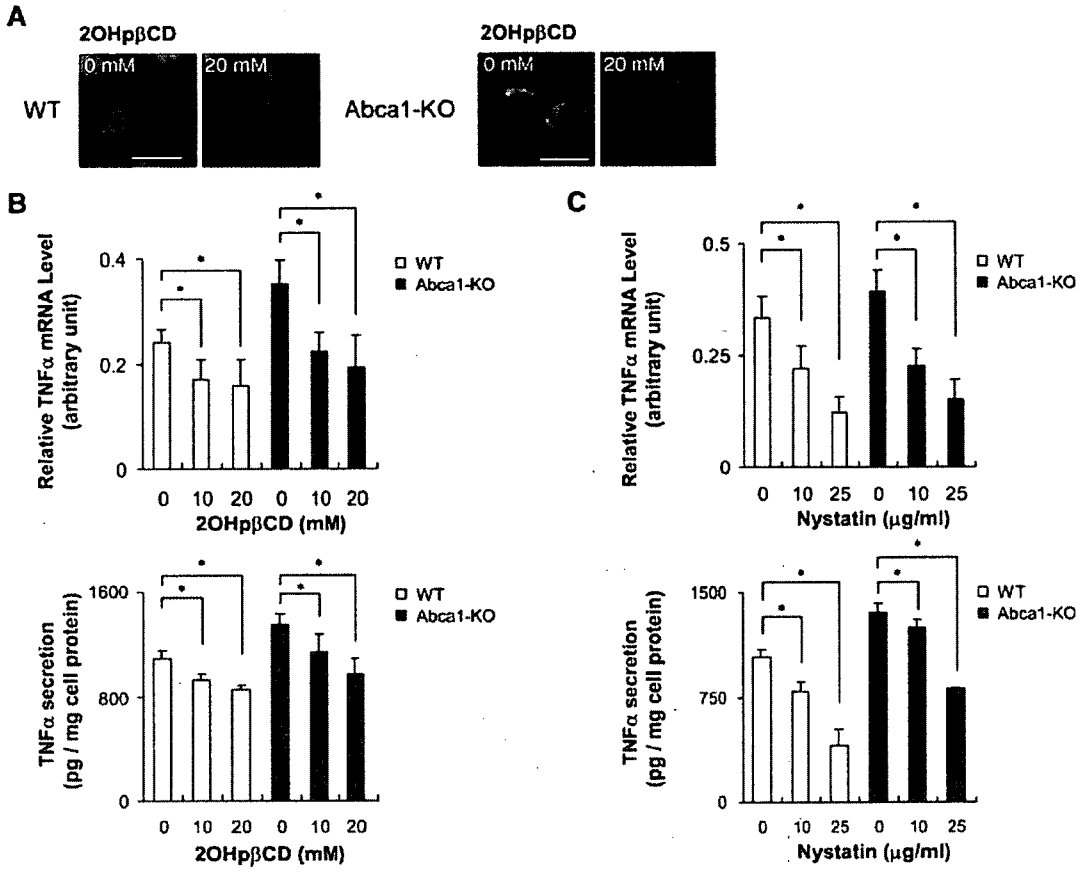

Fig. 4. Effect of lipid raft modulators on mRNA and secretion of TNF-α. A: To deplete cholesterol from lipid rafts, the macrophages were treated with 2-hydroxypropyl-β-cyclodextrin (2OHpβCD) (18847-64; Nacalai Tesque) for 30 min on ice. After treatment, the Abca1-KO and WT macrophages were stained with 10 μg/ml BCθ and streptavidin-Alexa Flour 594 conjugate, as described in Methods (red). The nuclei were stained with 4′,6-diamino-phenylindole (blue). Images were acquired by confocal laser microscopy. Bars = 10 μm. B: After treatment with 2OHpβCD for 30 min, the Abca1-KO and WT macrophages were stimulated by 10 ng/ml LPS at 37°C. TNF-α mRNA levels after 30 min and TNF-α secretion into the medium during 1 h were quantified, as described in Methods. C: To disrupt cholesterol-rich domains, the Abca1-KO and WT macrophages were treated with nystatin (N-6261; Sigma-Aldrich) for 5 min on ice. After treatment with nystatin, the macrophages were stimulated by 10 ng/ml LPS at 37°C. TNF-α mRNA levels after 30 min and TNF-α secretion into the medium during 1 h were measured. Mean and SD values were calculated from the data from three independent experiments. * $P < 0.05$ by Student's *t*-test.

Abca1 deficiency may accelerate atherosclerosis mediated by the increase of lipid rafts

TD is a familial HDL deficiency, which is a model for impaired cholesterol efflux, the initial step of RCT, and is frequently associated with cardiovascular diseases. We previously reported that a patient with TD suffered from severe coronary atherosclerosis using intravascular ultrasonography (9). Many previous studies have indicated that TD is associated with mutations in the Abca1 gene and that the loss of function of Abca1 led to defective cholesterol and phospholipid efflux from macrophages, followed by intracellular lipid accumulation, foam cell formation, and atherosclerosis (**Fig. 5**, left). In this study, we have shown another aspect of TD: that impaired cholesterol efflux may cause the deposition of free cholesterol in lipid rafts (Fig. 5, right) and that the increased lipid rafts may play a principal role in the regulation of the acute response of TNF-α to LPS stimulation. These observations may indicate that premature atherosclerosis in patients with TD may be accelerated by enhanced inflammation through an abnormality of lipid rafts. In vivo, the increased TNF-α levels in the plasma of Abca1-KO mice or TD patients have not been reported. Further studies will be necessary to clarify this issue.

During the preparation of our manuscript, Landry et al. (37) reported the unique relationship between Abca1 expression and membrane microdomains. They used BHK cells expressing a functional Abca1 or a nonfunctional Abca1 with a mutation in the ATP binding domain. They clearly showed that the overexpression of Abca1 results in the disruption of microdomains through its ATPase-related functions. On the other hand, we focused on the cause of TD and independently investigated the macrophages derived from a patient with TD and Abca1-KO mice. We demonstrated the increase in lipid rafts with two newly developed probes recognizing cholesterol directly

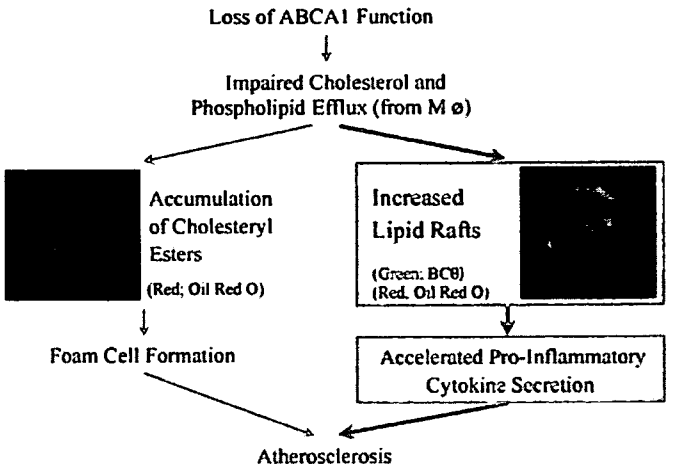

Fig. 5. A novel phenotype may accelerate atherosclerosis in Abca1-KO macrophages. Many studies have indicated that the loss of function of Abca1 causes the defective cholesterol and phospholipid efflux from macrophages, followed by the accumulation of cholesteryl esters, foam cell formation, and atherosclerosis. In this study, we revealed another novel phenotype of Abca1 deficiency: that impaired cholesterol efflux may influence plasma membrane lipid composition. Increased lipid rafts represent an important platform for the LPS-induced response and an accelerated proinflammatory cytokine release. Double staining with Oil Red O (red) and BCθ (green) made it possible to show cell surface free cholesterol and intracellular cholesteryl esters (lipid droplets) simultaneously and distinctly. Both panels show human monocyte-derived macrophages from a patient with TD.

and suggested accelerated TNF-α secretion under Abca1-KO conditions. Together, these data strongly demonstrate that Abca1 might be involved in the regulation and formation of lipid rafts in plasma membranes.

Cholesterol deposition and inflammation in macrophages

It is widely believed that inflammation might contribute to the progression of atherosclerosis. However, the relationship between intracellular lipid storage and inflammation in macrophages has not been clarified. Some studies revealed the relationship between cholesterol deposition and cytokine secretion in macrophages. Li et al. (38) demonstrated that TNF-α and interleukin-6 were induced in free cholesterol-loaded macrophages without LPS stimulation. They speculated that an excess storage of endoplasmic reticulum cholesterol may be the cause. Our data raised the possibility that cholesterol deposition in plasma membranes might affect the accelerated induction of TNF-α. On the other hand, Francone et al. (39) reported an observational study about the intracellular lipid storage and proinflammatory conditions of Abca1 and LDL receptor double knockout macrophages. In our study, we revealed one of the molecular mechanisms for this, showing that the increased lipid rafts may result in abnormal cytokine release.

Lipid rafts as a therapeutic target

Abca1 plays a key role in the regulation of cholesterol homeostasis and the function of macrophages. We demonstrated the relationship between Abca1 and lipid rafts using Abca1-defective animal and human models. On the other hand, in Abca1-expressing macrophages, the function of Abca1 was altered under some conditions. Wang and Oram (40, 41) reported that unsaturated fatty acids reduced Abca1 expression in macrophages by enhancing its degradation rate. These findings might support the speculation that the Abca1 of normal macrophages might be destabilized by unsaturated fatty acids, resulting in alterations of lipid rafts. The alteration of lipid rafts should be investigated in other atherogenic conditions affecting lipid efflux. In this study, we demonstrated that an extremely short-time modification of lipid composition in plasma membranes, using lipid raft modulators, might be a novel therapeutic strategy to attenuate acute accelerated proinflammatory events in macrophages.

Conclusion

Abca1-KO macrophages with defective lipid efflux exhibited increased lipid rafts on the cell surface and accelerated TNF-α release, which is a novel phenotype of macrophages with defective lipid efflux. Thus, modulation of Abca1 and lipid rafts may become a novel therapeutic target to prevent atherosclerosis.

This work was supported by Grants-in-Aid 11557055 and 10671070 to S.Y. and 13671191 to K-i.H. from the Ministry of Education, Science, Sports, and Culture of Japan. This work was also supported by a grant from the Japan Society for the Promotion of Science to S.Y. and Z. Zhang. This research was partially supported by an International HDL Research Awards Program grant from Pfizer, a grant from the Novartis Foundation for Gerontological Research, a grant from the Takeda Medical Research Foundation, and a grant from the Ono Medical Foundation to S.Y.

REFERENCES

1. Glomset, J. A. 1968. The plasma lecithin:cholesterol acyltransferase reaction. *J. Lipid Res.* **9**: 155–167.
2. Hirano, K., F. Matsuura, K. Tsukamoto, Z. Zhang, A. Matsuyama, K. Takaishi, R. Komuro, T. Suehiro, S. Yamashita, Y. Takai, et al. 2000. Decreased expression of a member of the Rho GTPase family, Cdc42Hs, in cells from Tangier disease—the small G protein may play a role in cholesterol efflux. *FEBS Lett.* **484**: 275–279.
3. Zhang, Z., K. Hirano, K. Tsukamoto, C. Ikegami, M. Koseki, K. Saijo, T. Ohno, N. Sakai, H. Hiraoka, I. Shimomura, et al. 2005. Defective cholesterol efflux in Werner syndrome fibroblasts and its phenotypic correction by Cdc42, a RhoGTPase. *Exp. Gerontol.* **40**: 286–294.
4. Tsukamoto, K., K. Hirano, K. Tsujii, C. Ikegami, Z. Zhang, Y. Nishida, T. Ohama, F. Matsuura, S. Yamashita, and Y. Matsuzawa. 2001. ATP-binding cassette transporter-1 (ABCA1) induces rear-

JOURNAL OF LIPID RESEARCH

rangement of actin cytoskeletons possibly through Cdc42/N-WASP. *Biochem. Biophys. Res. Commun.* **287:** 757–765.
5. Hirano, K., S. Yamashita, Y. Nakagawa, T. Ohya, F. Matsuura, K. Tsukamoto, Y. Okamoto, A. Matsuyama, K. Matsumoto, J. Miyagawa, et al. 1999. Expression of human scavenger receptor class B type I in cultured human monocyte-derived macrophages and atherosclerotic lesions. *Circ. Res.* **85:** 108–116.
6. Assmann, G., A. Eckardstein, and H. B. Brewer. 2001. Familial analphalipoproteinemia: Tangier disease. *In* Metabolic and Molecular Bases of Inherited Diseases. 8th edition. Vol. 2. McGraw Hill, New York. 2937–2960.
7. Oram, J. F., and S. Yokoyama. 1996. Apolipoprotein-mediated removal of cellular cholesterol and phospholipids. *J. Lipid Res.* **37:** 1503–1521.
8. Nishida, Y., K. Hirano, K. Tsukamoto, M. Nagano, C. Ikegami, K. Roomp, M. Ishihara, N. Sakane, Z. Zhang, K. Tsujii, et al. 2002. Expression and functional analyses of novel mutations of ATP-binding cassette transporter-1 in Japanese patients with high-density lipoprotein deficiency. *Biochem. Biophys. Res. Commun.* **290:** 713–721.
9. Komuro, R., S. Yamashita, S. Sumitsuji, K. Hirano, T. Maruyama, M. Nishida, F. Matsuura, A. Matsuyama, T. Sugimoto, N. Ouchi, et al. 2001. Tangier disease with continuous massive and longitudinal diffuse calcification in the coronary arteries: demonstration by the sagittal images of intravascular ultrasonography. *Circulation.* **101:** 2446–2448.
10. Brooks-Wilson, A., M. Marcil, S. M. Clee, L. H. Zhang, K. Roomp, M. V. Dam, L. Yu, C. Brewer, J. A. Collins, H. O. Molhuizen, et al. 1999. Mutations in ABC1 in Tangier disease and familial high-density lipoprotein deficiency. *Nat. Genet.* **22:** 336–345.
11. Bodzioch, M., E. Orso, J. Klucken, T. Langmann, A. Bottcher, W. Diederich, W. Drobnik, S. Barlage, C. Buchler, M. Porsch-Ozcurumez, et al. 1999. The gene encoding ATP-binding cassette transporter 1 is mutated in Tangier disease. *Nat. Genet.* **22:** 347–351.
12. Rust, S., M. Rosier, H. Funke, J. Real, Z. Amoura, J. C. Piette, J. F. Deleuze, H. B. Brewer, N. Duverger, P. Denefle, et al. 1999. Tangier disease is caused by mutations in the gene encoding ATP-binding cassette transporter 1. *Nat. Genet.* **22:** 352–355.
13. Pike, L. J. 2006. Rafts defined: a report on the Keystone symposium on lipid rafts and cell function. *J. Lipid Res.* **47:** 1597–1598.
14. Simons, K., and E. Ikonen. 1997. Functional rafts in cell membranes. *Nature.* **387:** 569–572.
15. Anderson, R. G., and K. Jacobson. 2002. A role for lipid shells in targeting proteins to caveolae, rafts, and other lipid domains. *Science.* **296:** 1821–1825.
16. Drobnik, W., H. Borsukova, A. Bottcher, A. Pfeiffer, G. Liebisch, G. J. Schutz, H. Schindler, and G. Schmitz. 2002. Apo AI/ABCA1-dependent and HDL3-mediated lipid efflux from compositionally distinct cholesterol-based microdomains. *Traffic.* **3:** 268–278.
17. Macdonald, J. L., and L. J. Pike. 2005. A simplified method for the preparation of detergent-free lipid rafts. *J. Lipid Res.* **46:** 1061–1067.
18. Gaus, K., M. Rodriguez, K. R. Ruberu, I. Gelissen, T. M. Sloane, L. Kritharides, and W. Jessup. 2005. Domain-specific lipid distribution in macrophage plasma membranes. *J. Lipid Res.* **46:** 1526–1538.
19. Li, Q., M. Wang, L. Tan, C. Wang, J. Ma, N. Li, Y. Li, G. Xu, and J. Li. 2005. Docosahexaenoic acid changes lipid composition and interleukin-2 receptor signaling in membrane rafts. *J. Lipid Res.* **46:** 1904–1913.
20. Urano, Y., I. Hayashi, N. Isoo, P. C. Reid, Y. Shibasaki, N. Noguchi, T. Tomita, T. Iwatsubo, T. Hamakubo, and T. Kodama. 2005. Association of active gamma-secretase complex with lipid rafts. *J. Lipid Res.* **46:** 904–912.
21. Waheed, A. A., Y. Shimada, H. F. G. Heijen, M. Nakamura, M. Inomata, M. Hayashi, S. Iwashita, J. W. Slot, and Y. Ohno-Iwashita. 2001. Selective binding of perfringolysin O derivative to cholesterol-rich membrane microdomains (rafts). *Proc. Natl. Acad. Sci. USA.* **98:** 4926–4931.
22. Ohno-Iwashita, Y., Y. Shimada, A. A. Waheed, M. Hayashi, M. Inomata, M. Nakamura, M. Maruya, and S. Iwashita. 2004. Perfringolysin O, a cholesterol-binding cytolysin, as a probe for lipid rafts. *Anaerobe.* **10:** 125–134.
23. Reid, P. C., N. Sakashita, S. Sugii, Y. Ohno-Iwashita, Y. Shimada, W. F. Hickey, and T. Y. Chang. 2004. A novel cholesterol stain reveals early neuronal cholesterol accumulation in the Niemann-Pick type C1 mouse brain. *J. Lipid Res.* **45:** 582–591.
24. Ohno-Iwashita, Y., M. Iwamoto, S. Ando, and S. Iwashita. 1992. Effect of lipidic factors on membrane cholesterol topology: mode of binding of θ-toxin to cholesterol on liposomes. *Biochim. Biophys. Acta.* **1109:** 81–90.
25. Nakamura, M., H. Kondo, Y. Shimada, A. A. Waheed, and Y. Ohno-Iwashita. 2003. Cellular aging-dependent decrease in cholesterol in membrane microdomains of human diploid fibroblasts. *Exp. Cell Res.* **290:** 381–390.
26. Ishiwata, H., S. B. Sato, A. Vertut-Doi, Y. Hamashima, and K. Miyajima. 1997. Cholesterol derivative of poly (ethylene glycol) inhibits clathrin-independent, but not clathrin-dependent endocytosis. *Biochim. Biophys. Acta.* **1359:** 123–135.
27. Sato, S. B., K. Ishii, A. Makino, K. Iwabuchi, A. Yamaji-Hasegawa, Y. Senoh, I. Nagaoka, H. Sakuraba, and T. Kobayashi. 2004. Distribution and transport of cholesterol-rich membrane domains monitored by a membrane-impermeant fluorescent polyethylene glycol-derivatized cholesterol. *J. Biol. Chem.* **279:** 23790–23796.
28. Iwamoto, M., I. Morita, M. Fukuda, S. Murota, S. Ando, and Y. Ohno-Iwashita. 1997. A biotinylated perfringolysin O derivative: a new probe for detection of cell surface cholesterol. *Biochim. Biophys. Acta.* **1327:** 222–230.
29. McNeish, J., R. J. Aiello, D. Guyot, T. Turi, C. Gabel, C. Aldinger, K. L. Hoppe, M. L. Roach, L. J. Royer, J. Wet, et al. 2000. High density lipoprotein deficiency and foam cell accumulation in mice with targeted disruption of ATP-binding cassette transporter-1. *Proc. Natl. Acad. Sci. USA.* **97:** 4245–4250.
30. Ohama, T., K. Hirano, Z. Zhang, R. Aoki, K. Tsujii, Y. Nakagawa-Toyama, K. Tsukamoto, C. Ikegami, A. Matsuyama, M. Ishigami, et al. 2002. Dominant expression of ATP-binding cassette transporter-1 on basolateral surface of Caco-2 cells stimulated by LXR/RXR ligands. *Biochem. Biophys. Res. Commun.* **296:** 625–630.
31. Triantafilou, M., K. Miyake, D. T. Golenbock, and K. Triantafilou. 2002. Mediators of innate immune recognition of bacteria concentrate in lipid rafts and facilitate lipopolysaccharide-induced cell activation. *J. Cell Sci.* **115:** 2603–2611.
32. Murray, R. Z., F. G. Wylie, T. Khromykh, D. A. Hume, and J. L. Stow. 2005. Syntaxin 6 and Vti1b form a novel SNARE complex, which is up-regulated in activated macrophages to facilitate exocytosis of tumor necrosis factor-alpha. *J. Biol. Chem.* **280:** 10478–10483.
33. Brown, D. A., and J. K. Rose. 1992. Sorting of GPI-anchored proteins to glycolipid-enriched membrane subdomains during transport to the apical cell surface. *Cell.* **68:** 533–544.
34. Munro, S. 2003. Lipid rafts: elusive or illusive? *Cell.* **115:** 377–388.
35. Pike, L. J. 2003. Lipid rafts: bringing order to chaos. *J. Lipid Res.* **44:** 655–667.
36. Kay, J. G., R. Z. Murray, J. K. Pagan, and J. L. Stow. 2006. Cytokine secretion via cholesterol rich lipid raft associated SNAREs at the phagocytic cup. *J. Biol. Chem.* **281:** 11949–11954.
37. Landry, Y. D., M. Denis, S. Nandi, S. Bell, A. M. Vaughan, and X. Zha. 2006. ABCA1 expression disrupts raft membrane microdomains through its ATPase-related functions. *J. Biol. Chem.* In press.
38. Li, Y., R. F. Schwabe, T. D. Vries-Seimon, P. M. Yao, M-C. Gerbod-Giannone, A. R. Tall, R. J. Davis, R. Flavell, D. A. Brenner, and I. Tabas. 2005. Free cholesterol-loaded macrophages are an abundant source of tumor necrosis factor-α and interleukin-6. *J. Biol. Chem.* **280:** 21763–21772.
39. Francone, O. L., L. Royer, G. Boucher, M. Haghpassand, A. Freeman, D. Brees, and R. J. Aiello. 2005. Increased cholesterol deposition, expression of scavenger receptors, and response to chemotactic factors in Abca1-deficient macrophages. *Arterioscler. Thromb. Vasc. Biol.* **25:** 1198–1205.
40. Wang, Y., and J. F. Oram. 2002. Unsaturated fatty acids inhibit cholesterol efflux from macrophages by increasing degradation of ATP-binding cassette transporter A1. *J. Biol. Chem.* **277:** 5692–5697.
41. Wang, Y., and J. F. Oram. 2005. Unsaturated fatty acids phosphorylate and destabilize ABCA1 through a phospholipase D2 pathway. *J. Biol. Chem.* **280:** 35896–35903.

Clinical Chemistry 53:12
2128–2135 (2007)

Lipids, Lipoproteins, and Cardiovascular Risk Factors

Development of a Homogeneous Assay to Measure Remnant Lipoprotein Cholesterol

KAZUHITO MIYAUCHI,[1] NORIHIKO KAYAHARA,[2*] MASATO ISHIGAMI,[3] HIDEYUKI KUWATA,[4] HIDEHARU MORI,[4] HIROYUKI SUGIUCHI,[5] TETSUMI IRIE,[6] AKIRA TANAKA,[7] SHIZUYA YAMASHITA,[8] and TAKU YAMAMURA[3]

Background: **Quantification of triglyceride-rich lipoprotein (TRL) remnants is useful for risk assessment of coronary artery disease and the diagnosis of type III hyperlipoproteinemia. Although an immunoseparation procedure for remnant-like particle cholesterol has been evaluated extensively in recent years, available methods for measuring TRL remnants have not achieved wide use in routine laboratory practice, suggesting a need for a homogeneous assay that can measure TRL remnant cholesterol in serum or plasma without pretreatment.**

Methods: **We screened for suitable surfactants that exhibited favorable selectivity toward the VLDL remnant (VLDLR) fraction, including intermediate-density lipoproteins (IDLs). We investigated the principal characteristics of this assay by gel filtration of lipoproteins and their particle size distribution. We developed a simple assay and evaluated its performance with the Hitachi-7170 analyzer.**

Results: **Polyoxyethylene-polyoxybutylene block copolymer (POE-POB) exhibited favorable selectivity toward VLDLR and IDL fractions. POE-POB removed apolipoprotein (apo) E and apo C-III from IDL particles in the presence of cholesterol esterase (CHER), and the particle size distribution of IDLs became smaller after the reaction. These results revealed that IDL particles are specifically modified in the presence of CHER and POE-POB, making their component cholesterol available for enzymatic assay. Addition of phospholipase D improved the reactivity toward chylomicron remnants (CMRs). We found a high correlation [$y = 1.018x - 0.01$ mmol/L, $r = 0.962$ (n = 160)] between the proposed assay and the immunoseparation assay in serum from healthy individuals.**

Conclusion: **The homogeneous assay described in this report can measure TRL remnant cholesterol, including CMRs, VLDLRs, and IDLs, with high sensitivity and specificity.**

Previous clinical and experimental studies have suggested that triglyceride-rich lipoprotein (TRL)[9] remnants play an important role in atherogenesis *(1)*. It has also been reported that postprandial hyperlipidemia induces fat accumulation in arterial walls *(2)* and is strongly associated with the progression of coronary artery disease (CAD) *(3)*. Many studies have shown a high correlation between postprandial hyperlipidemia and atherosclerosis *(4, 5)*. In addition, the Montreal Heart Study showed an independent contribution of increased VLDL remnants (VLDLRs) plus intermediate-density lipoproteins (IDLs) to the progression of CAD and related clinical events *(6)*. Furthermore, a report from the Framingham Heart Study found that remnant-like particle cholesterol (RLP-C),

[1] Scientific and Technical Affairs Department, Kyowa Medex Co., Ltd., Tokyo, Japan.
[2] Research and Development Department, Kyowa Medex Co., Ltd., Tokyo, Japan.
[3] Division of Health Sciences, Osaka University Graduate School of Medicine, Osaka, Japan.
[4] Research Laboratory Department, Kyowa Medex Co., Ltd., Shizuoka, Japan.
[5] Kumamoto Health Science University, Kumamoto, Japan.
[6] Faculty of Medical and Pharmaceutical Sciences, Kumamoto University, Kumamoto, Japan.
[7] Laboratory of Clinical Nutrition and Medicine, Kagawa Nutrition University, Saitama, Japan.
[8] Department of Cardiovascular Medicine, Osaka University Graduate School of Medicine, Osaka, Japan.
* Address correspondence to this author at: Research and Development Department, Kyowa Medex Co., Ltd., 1-8-10, Harumi, Chuo-ku, Tokyo 104-6004, Japan. Fax 81-3-6219-7614; e-mail norihiko.kayahara@kyowa.co.jp.
Received May 21, 2007; accepted September 5, 2007.
Previously published online at DOI: 10.1373/clinchem.2007.092296

[9] Nonstandard abbreviations: TRL, triglyceride-rich lipoprotein; CAD, coronary artery disease; VLDLR, VLDL remnant; IDL, intermediate-density lipoprotein; RLP-C, remnant-like particle cholesterol; apo, apolipoprotein; CM, chylomicron; LPL, lipoprotein lipase; CMR, CM remnant; TG, triglyceride; PL-D, phospholipase D; CHER, cholesterol esterase; CHOD, cholesterol oxidase; POE-POB, polyoxyethylene-polyoxybutylene block copolymer.

which provides an estimate of TRL remnants, is an independent risk factor for CAD in women *(7)*.

TRL remnants are metabolic intermediates formed when apolipoprotein (apo) B-48–containing chylomicrons (CMs) of intestinal origin and apo B-100–containing VLDL of hepatic origin are hydrolyzed by lipoprotein lipase (LPL) on the surface of vascular endothelium; they are referred to as CM remnants (CMRs) and VLDLRs, respectively *(8)*. VLDLRs are found not only in TRL ($d <$ 1.006 kg/L), but also in IDLs (1.006 to 1.019 kg/L). Therefore IDLs are also referred to as remnants *(1)*. Compared with nascent VLDLs and CMs, TRL remnants and IDLs contain fewer triglycerides (TGs) and phospholipids, but relatively more esterified cholesterol and apo E *(9–12)*. TRL remnants have been identified, isolated, and quantified in plasma on the basis of their density, charge, size, specific lipid components, apo composition, or apo immunospecificity *(1, 13)*. Major methods include ultracentrifugation for IDLs *(14, 15)*; agarose gel electrophoresis for β-VLDLs and slow pre-β VLDLs and PAGE for IDLs (presence or absence of a midband) *(11, 14, 16)*; and immunoseparation for RLP-C as an unbound fraction not adsorbed by anti–apo A-I or anti–apo B-100 antibodies *(17, 18)*. These methods require special equipment and are time-consuming; hence, they are not well suited as routine tests in hospitals and clinics. There is a need for a simple, rapid, automated method to quantify TRL remnants in serum or plasma.

Specific interaction of surfactants with lipoproteins has been successfully used for developing direct lipoprotein cholesterol assays, in which the surfactants are able to recognize differences in hydrated density, net charge, or size of the various lipoprotein fractions *(19, 20)*. We have therefore attempted to establish a new homogeneous assay for remnant lipoprotein cholesterol that can be carried out by using a universal autoanalyzer without any pretreatment. Herein we describe such an assay for remnant lipoprotein cholesterol by use of a synthetic nonionic surfactant and phospholipase D (PL-D).

Materials and Methods

MATERIALS

We used cholesterol esterase (CHER) (EC3.1.1.34: 134 kDa, *Pseudomonas* species) from Toyobo, cholesterol oxidase (CHOD) (EC1.1.3.6: 58 kDa, recombinant *Escherichia coli*) from Kyowa Hakko, PL-D (EC3.1.4.4: 46 kDa, *Streptomyces* species) from Asahi Kasei, Good's buffer MOPS from Dojindo Laboratories, 4-aminoantipyrine from Kanto Chemical, and *N*-ethyl-*N*-(3-methylphenyl)-*N'*-succinylethylenediamine manufactured by Kyowa Medex. Polyoxyethylene-polyoxybutylene block copolymer (POE-POB) was obtained from NOF Corporation, and the immunoseparation reagents for RLP-C measurements were obtained from Otsuka Pharmaceutical. Human serum samples were obtained from 160 healthy volunteers (100 men and 60 women, age 20 to 59 years) who had fasted for 12 h and from hyperlipidemic patients with the approval of ethics committees at Osaka University School of Medicine and Tokyo Medical and Dental University. We used hyperlipidemic sera for lipoprotein fractions isolated by ultracentrifugation to obtain VLDL (0.96–1.006 kg/L), IDL (1.006–1.019 kg/L), LDL (1.019–1.063 kg/L), and HDL (1.063–1.021 kg/L) fractions *(15, 21, 22)*. Blood was collected in plastic serum tubes (Venoject II; inner diameter 12 mm; length 10 cm; with procoagulant agent; Terumo).

SEPARATION OF LIPOPROTEINS BY ULTRACENTRIFUGATION AND GEL FILTRATION

The density of fasting serum obtained from a patient with type III hyperlipoproteinemia (apo E phenotype E2/2) was adjusted to 1.006 and 1.019 kg/L, and the treated serum was ultracentrifuged at 131 918*g* for 20 h (Beckman: 50.4 Ti rotor). We collected the supernatant fraction after tube-slicing with Pasteur pipette to obtain lipoprotein fractions with densities of <1.006 kg/L and <1.019 kg/L. For separation of lipoprotein fractions, we used Superose 6 HR 10/30 columns (bed volume 24 mL; inner diameter 10 mm; length 30 cm; count 2 columns; Pharmacia) *(23, 24)*. Each lipoprotein fraction was eluted with 0.15 mol/L NaCl and 1 mmol/L EDTA (pH 7.4) at a flow rate of 0.3 mL/min. We collected the column effluent in 0.5-mL fractions, in which total cholesterol concentration was measured by enzymatic assay (Kyowa Medex) and apo E concentration was measured by immunoturbidimetric assay (Daiichi Pure Chemicals).

CHARACTERIZATION BY GEL FILTRATION ANALYSIS

We added a mixture of POE-POB 12 g/L, CHER 1.5 kU/L, and MOPS buffer 20 mmol/L, pH 6.5, as the reaction reagent to the IDL, LDL, and HDL fractions obtained by ultracentrifugation at a 1:1 ratio, and mixtures were then incubated at 37 °C for 5 min. For gel filtration analysis of the reaction mixture, we used Superose 6 HR 10/30 columns *(23, 24)*. With each sample, 0.2 mL was applied with 0.15 mol/L NaCl and 1 mmol/L EDTA (pH 7.4) at a flow rate of 0.5 mL/min, and 0.2-mL fractions were collected. Concentrations of total cholesterol and TGs in the fractions were measured by enzymatic assay (Kyowa Medex), and the concentrations of apo E, apo C-III, apo B, and apo A-I were measured by immunoturbidimetric assay (Daiichi Pure Chemicals). For gel filtration analysis of serum samples obtained after feeding a high-fat meal, we used TSK gel Lipopropak XL columns (inner diameter 7.8 mm; length 30 cm; count 2; Tosoh) *(24, 25)*. A postprandial serum sample was obtained from a single individual 10 h after a high-fat meal containing 100 g of fat and 75 g of alcohol. Of the serum sample, 0.2 mL was subjected to gel filtration with 0.15 mol/mL NaCl and 1 mmol/mL EDTA (pH 7.4) at a flow rate of 0.5 mL/min, and 0.2-mL fractions were collected. Concentrations of total cholesterol, TGs, apo E, apo C-III, and apo B were measured as described above, and apo B-48 was measured by chemiluminescence enzyme immunoassay (Fujirebio).

CHARACTERIZATION BY PARTICLE SIZE DISTRIBUTION ANALYSIS

For analysis of lipoprotein size distribution, we used a fiber optic dynamic light-scattering photometer (particle size range from 3 nm to 3 μm; FDLS-3000, Otsuka Electronics). The VLDL, IDL, LDL, and HDL fractions obtained by ultracentrifugation were mixed with the reaction reagent at a 1:1 ratio, incubated at 37 °C for 0 to 9 min, and diluted 100-fold for testing.

ANALYTICAL PROCEDURE

For the measurement of remnant lipoprotein cholesterol, the final formulation of the 1st reagent was *N*-ethyl-*N*-(3-methylphenyl)-*N'*-succinylethylenediamine (1.1 mmol/L), POE-POB (8 g/L), and MOPS buffer (20 mmol/L, pH 6.5); that of the 2nd reagent was PL-D (8 kU/L), CHER (1.5 kU/L), CHOD (3 kU/L), peroxidase (20 kU/L), 4-aminoantipyrine (2.5 mmol/L), and MOPS buffer (20 mmol/L, pH 6.8).

Serum samples were stored at 4 °C after collection and were subjected to testing (Hitachi-7170 autoanalyzer) within 2 days, within which time the values obtained by the assay were stable. To 3.8 μL of each serum sample, we added 180 μL of the 1st reagent and incubated the resulting solution at 37 °C for 5 min. Next, we added 60 μL of the 2nd reagent and incubated the reaction mixture at 37 °C for 5 min. The chromophore formed in a coupled reaction with peroxidase was measured spectrophotometrically at dual wavelengths of 600 nm (main) and 700 nm (subsidiary), and the end-point method was used for the calculation. A serum-base calibrator prepared from TG-rich human sera (Kyowa Medex, 0.592 mmol/L) was used to estimate remnant lipoprotein cholesterol. We performed the RLP-C immunoseparation method according to the package insert provided by Otsuka Pharmaceutical, and serum samples were stored at 4 °C after collection and tested within 2 days. For PAGE, Lipophor (Jokoh) was used. The total imprecision (CV) of the methods was as follows: total cholesterol <1.2%, TG <1.1%, apo A1 <5%, apo CIII <5%, apo E <5%, apo B <5%, and apo B-48 <6.4%. The intraassay imprecision (CV) of the immunoseparation method was <15%.

STATISTICS

We used Pearson correlation coefficient analysis and simple regression to assess the relation between the proposed assay and the immunoseparation assay. Statistical analysis was performed with Excel 2003 (Microsoft) with the add-in software Statcel 2 *(26)*.

Results

SEPARATION OF LIPOPROTEINS BY ULTRACENTRIFUGATION AND GEL FILTRATION AND SELECTION OF SURFACTANT

To obtain the VLDLR fraction from the serum of a patient with type III hyperlipoproteinemia, we conducted ultracentrifugation and gel filtration. Fig. 1 shows the gel filtration profile of the lipoproteins from the patient serum. Whereas the main peak of the VLDL fraction is ordinarily detected at void volume *(24)*, that of the $d <$ 1.006 kg/L fraction from the patient was detected at void volume and at a smaller particle size. Compared with the void volume fraction, the smaller peak contained more apo E. Because the density of IDL is 1.006 to 1.019 kg/L, IDL elution can be identified by subtracting the concentration of the $d <$ 1.006 kg/L fraction from that of the $d <$ 1.019 kg/L fraction (Fig. 1). The smaller VLDL particle size area of the gel filtration ($d <$ 1.006 kg/L) mostly overlapped with the elution profile of IDL. In the present study, the fractions 14 through 19 from the $d <$ 1.019 kg/L fraction, as shown in Fig. 1, which were considered to contain VLDLR including IDL, were mixed to become the VLDLR fraction.

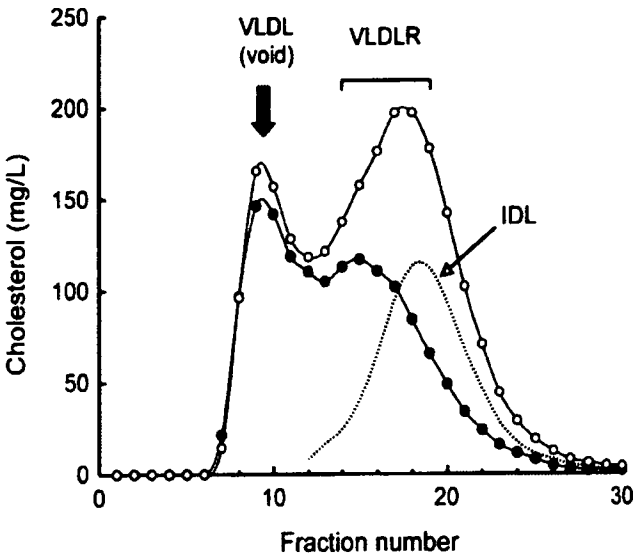

Fig. 1. Gel filtration profile of the $d <$ 1.019 (VLDL+IDL) and $d <$ 1.006 (VLDL) fractions from a patient serum with type III hyperlipoproteinemia fractionated by Superose 6 HR 10/30 columns.

○, total cholesterol in $d <$1.019; ●, total cholesterol in d <1.006; *dotted line*, IDL cholesterol calculated by difference.

We examined 180 surfactants with diverse structures, with which selectivity toward cholesterol in VLDLRs was investigated. Of the surfactants tested, POE-POB of 10 042 Da (see Supplemental Data Fig. 1), which has relatively high solubility as well as high selectivity toward cholesterol in VLDLRs, was selected for further consideration.

EFFECTS OF POE-POB ON GEL FILTRATION OF LIPOPROTEINS AND THEIR SIZE DISTRIBUTION

Using gel filtration and size distribution studies, we gained insight into the mechanism by which POE-POB exhibits its selectivity toward VLDLRs. Fig. 2A shows the profiles of cholesterol, TGs, apo B, apo E, and apo C-III after applying the IDL fraction to gel filtration obtained by ultracentrifugation. Total cholesterol, TGs, apo B,

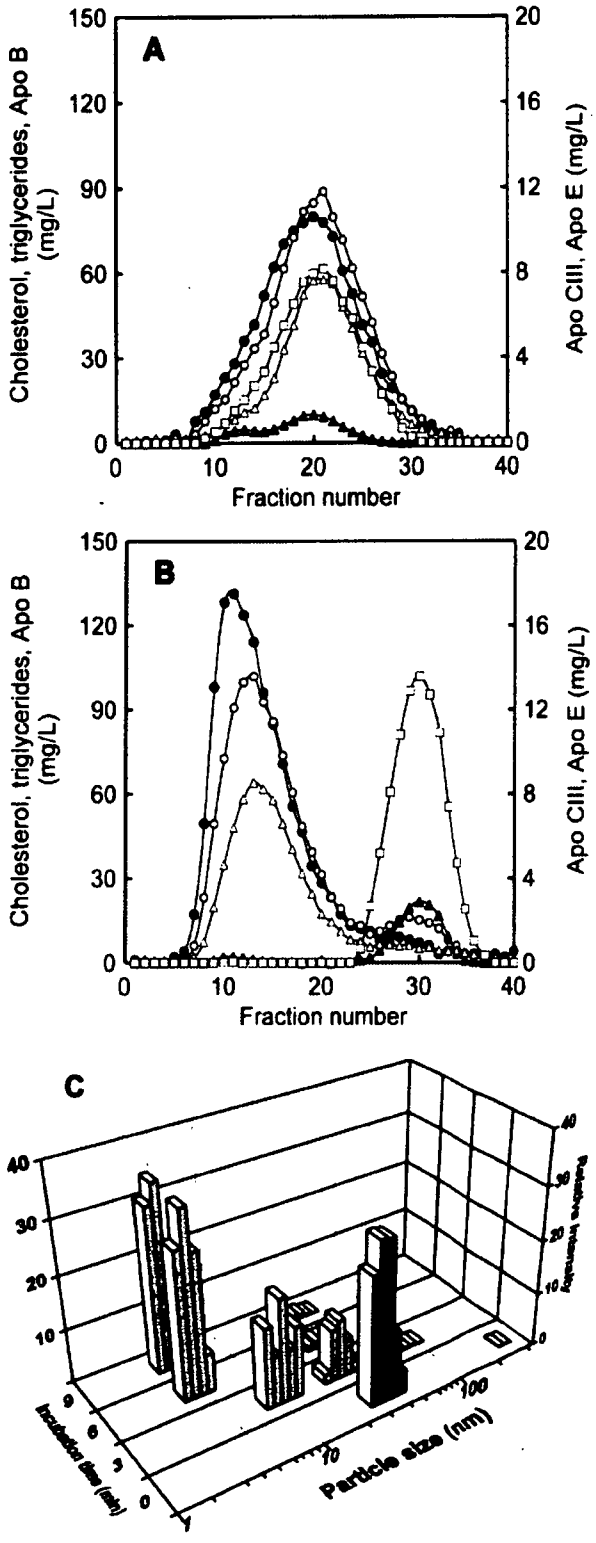

Fig. 2. Effect of POE-POB on gel filtration profile of IDL fraction fractionated on Superose 6 HR 10/30 columns and its particle size distribution.

(*A*), IDL fraction without POE-POB. (*B*), IDL fraction with POE-POB. ○, total cholesterol; ●, TGs; △, apo B; ▲, apo E; □, apo CIII. (*C*), particle size distribution of IDL fractions before (0) and 3, 6, and 9 min after adding POE-POB.

apo E, and apo C-III were eluted at mostly the same retention time. Next, the IDL fraction was mixed with the reaction reagents at a 1:1 ratio, incubated at 37 °C for 5 min, and applied to gel filtration (Fig. 2B). When comparing the retention times of apos, apo B was eluted at approximately the same time as total cholesterol and TGs, but apo E and apo C-III were eluted with significant delay. When LDLs and HDLs were analyzed by the same methods, in contrast to IDLs, different apo peaks were not seen before and after the reaction reagent treatment.

We examined the effect of POE-POB on the size distribution of lipoprotein fractions by use of a fiber optic dynamic light-scattering photometer (FDLS-3000), which quantifies particle size based on light scattering. As shown in Fig. 2C, the particle size of the IDL fraction decreased with time after mixing with the reaction reagent. By contrast, changes in particle sizes of the VLDL, LDL, and HDL fractions were relatively small, particularly with LDL and HDL.

IMPROVED REACTIVITY TO CMRS

With the reagent containing POE-POB (8 g/L), which exhibited a high selectivity toward VLDLR in the presence of CHER (1.5 kU/L) and CHOD (3 kU/L), the correlation with the immunoseparation method for RLP-C was investigated using serum samples, including those with high TG concentrations. The results showed poor correlations with nonfasting samples having high TG concentrations. To clarify the cause of the differences, detailed reactivity was compared using lipoproteins isolated by gel filtration (*24*, *25*). A serum sample collected from an individual after a high-fat meal was subjected to gel filtration. Fig. 3A shows gel filtration profiles of lipids and apos. Large CMs were eluted in the void volume (*25*), but apo B-48 and apo E were observed mostly in smaller particles, thus suggesting the presence of CMRs. Next, in the presence of CHER (1.5 kU/L) and CHOD (3 kU/L), the reactivity of reagent containing POE-POB (8 g/L) toward CMRs was examined, but the reactivity was very low in the region corresponding to CMRs. This low reactivity toward CMRs was thought to be the cause of the differences with the immunoseparation method, which detects all particles containing apo B-48. Therefore, PL-D (5 kU/L) was added to the reagent containing POE-POB (8 g/L) in the presence of CHER (1.5 kU/L) and CHOD (3 kU/L), and the reactivity of the fractions containing CMR significantly improved (Fig. 3A). As shown in Fig. 3B, the reagent containing POE-POB and PL-D in the presence of CHER and CHOD exhibited the required selectivity toward cholesterol in VLDLRs, including IDL, when a serum from a patient with type III hyperlipoproteinemia was used. The above results confirmed that the proposed assay made it possible to detect cholesterol in CMRs, VLDLRs, and IDLs.

LINEARITY STUDY AND LOWER LIMIT OF DETECTION

Five serum samples were diluted with 155 mmol/L NaCl, and linearity of the method was examined. The linearity was obtained up to 2.1 mmol/L cholesterol. The lower detection limit was 0.005 mmol/L.

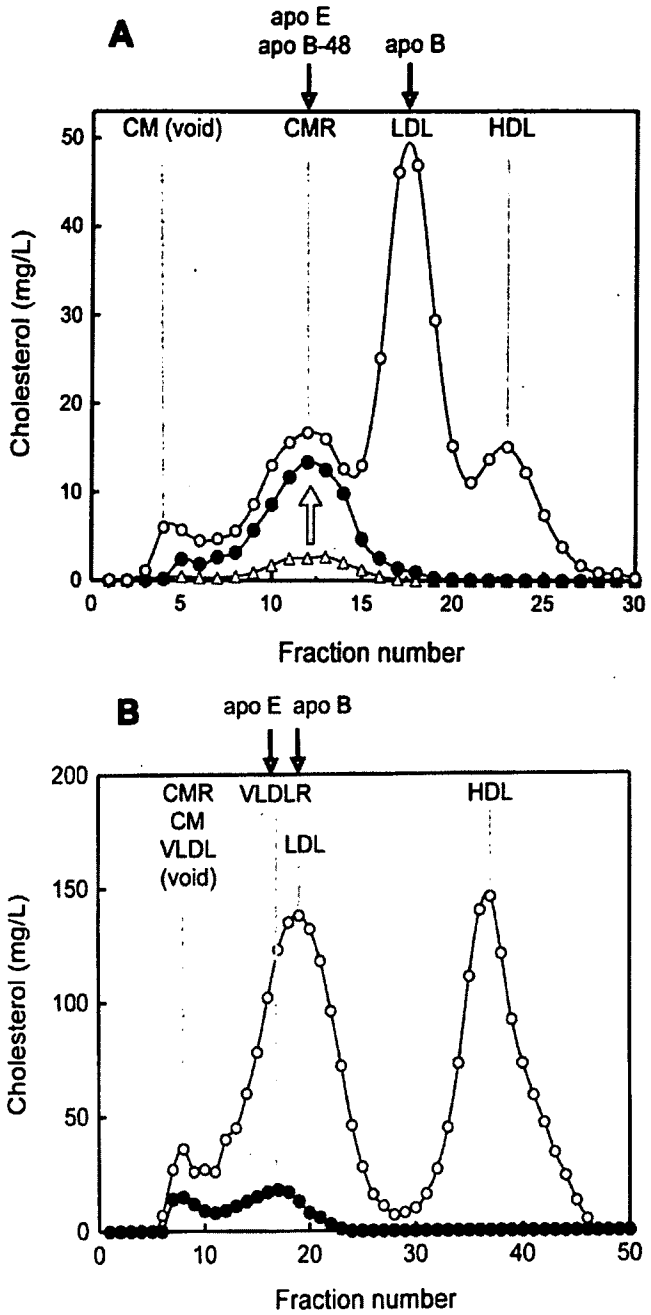

Fig. 3. Gel filtration profiles of serum obtained after a high-fat meal in the presence and absence of PL-D in reaction reagents (*A*) and those of a patient serum with type III hyperlipoproteinemia (*B*).

TSK gel Lipopropak XL columns and Superose 6 HR 10/30 columns were used in *A* and *B*, respectively. ○, total cholesterol; △, cholesterol detected by reagent containing [CHER (1.5 kU/L) + CHOD (3 kU/L) + POE-POB (8 g/L)]; ●, cholesterol detected by reagent containing [CHER (1.5 kU/L) + CHOD (3 kU/L) + POE-POB (8 g/L) + PL-D (8 kU/L)]; *downward arrows*, location of apos; *upward arrow*, improvement of reactivity of cholesterol in CMRs.

IMPRECISION

The within-run imprecision (CV) of the method was 1.25% at 0.100 mmol/L, 0.96% at 0.317 mmol/L, and 1.8% at 0.412 mmol/L. The run-to-run imprecision (CV) of the method was 2.75% at 0.111 mmol/L, 1.54% at 0.199 mmol/L, and 1.59% at 0.499 mmol/L.

EFFECTS OF INTERFERING SUBSTANCES

To pooled serum samples, we added conjugated bilirubin (up to 0.68 mmol/L), free bilirubin (up to 0.68 mmol/L), hemoglobin (up to 4.9 g/L), and Intrafat (up to 10%) (Nihon Seiyaku Kogyo). None of these compounds produced more than a 5% error in the assay result.

COMPARISON WITH THE RLP-C IMMUNOSEPARATION METHOD

The proposed assay was compared with the immunoseparation method in fasting serum samples from 160 healthy volunteers. As shown in Fig. 4A, the regression equation for the comparison was $y = 1.018x - 0.01$ ($r = 0.96$). The mean (SD) of 160 sera was 0.18 (0.15) mmol/L for the immunoseparation method and 0.17 (0.16) mmol/L for the proposed method, respectively.

The relation with the immunoseparation method was also examined by use of sera from diabetic patients, which showed that the proposed method occasionally exhibited higher concentrations of remnant lipoprotein cholesterol than the immunoseparation method (Fig. 4B). When these samples were analyzed by PAGE, a large amount of midband *(14)* was detected, indicating increased concentrations of IDLs.

Discussion

Various methods have been developed to detect remnant lipoproteins in recent years. These methods are not well suited for use in regular laboratory practice because they are time-consuming and require special equipment. We used a special surfactant, POE-POB, and an enzyme, PL-D, to develop a homogenous assay that conveniently measures TRL remnant cholesterol in serum or plasma. The proposed assay does not require any sample pretreatment and uses 3.8 μL of serum, with the assay taking only 10 min on a regular autoanalyzer.

The proposed assay measures cholesterol in CMRs, VLDLRs, and IDLs by selectively modifying these 3 remnant lipoproteins with POE-POB and PL-D in the presence of CHER and CHOD. Polyoxamers including POE-POP have been successfully used as surface modifiers for improving the stability of latex particles *(27)* and as vehicles for transdermal drug delivery *(28)*. Furthermore, POE-POP, with a molecular weight of 3850 Da and a high polyoxypropylene content, was found to be LDL selective, and it has been used in assays for LDL cholesterol *(29)*.

POE-POB, with a molecular weight of 10 042 Da, was selected for this proposed assay. When the IDL fraction (VLDLRs) incubated with POE-POB in the presence of CHER was applied to gel filtration, apo E and apo C-III were eluted from gel filtration columns with significant delay compared with the retention time of total cholesterol, TGs, and apo B (Fig. 2, A and B). This result indicates that apo E and apo C-III were removed from the

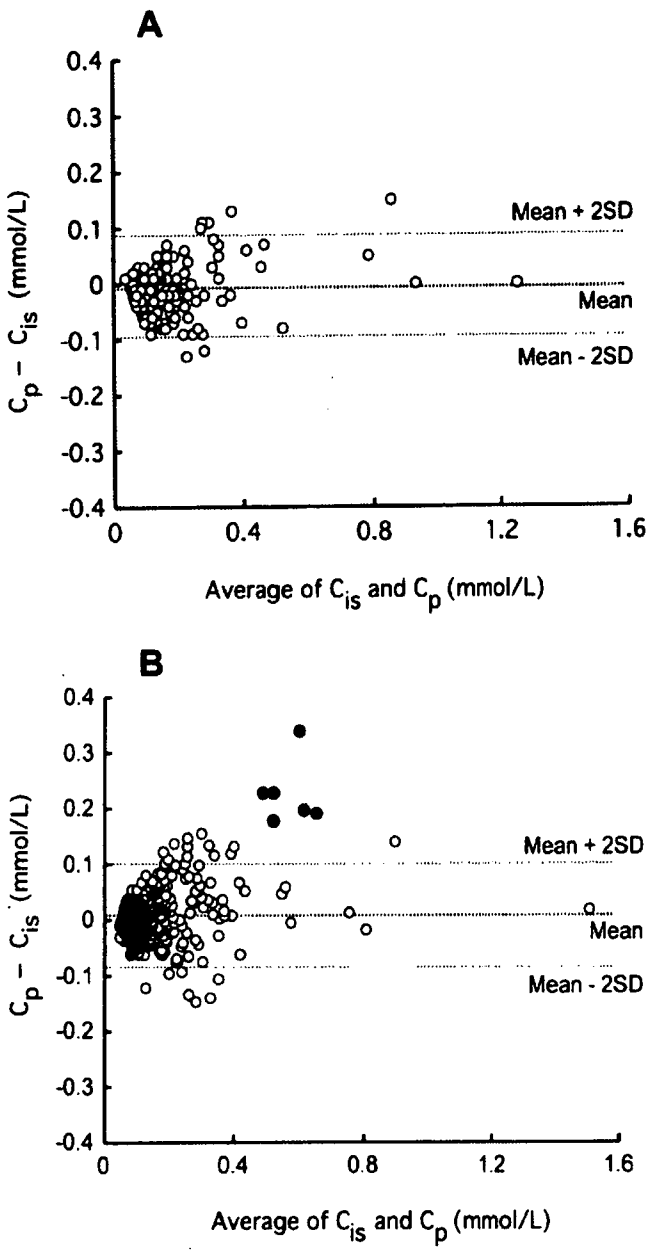

Fig. 4. Correlation between the immunoseparation method and the proposed method.

(*A*), Bland-Altman difference plot between the immunoseparation method (C_{is}) and the proposed method (C_p) in fasting serum samples from 160 healthy volunteers. (*B*), Bland-Altman difference plot between C_{is} and C_p in sera from diabetic patients. ●, samples in which the difference between C_{is} and C_p exceeded 0.17 mmol/L.

lipoprotein surfaces in the presence of CHER with POE-POB and formed isolated small particles. When treated with the reaction reagent, the elution time for IDL particles themselves was reduced. However, the size of IDLs treated with the reaction reagent became progressively smaller with time (Fig. 2C), suggesting that the interaction between the reaction reagent and IDL particles may affect the shape of IDL particles, thus increasing their apparent size. In addition, with the LDL and HDL fractions, small changes of elution time after reaction reagent addition also suggested changes in particle shape, but apo B in LDLs and apo A-I and apo E in HDLs were not removed from the respective lipoprotein particles.

Reaction reagent treatment also made IDLs smaller with time, thus clarifying that IDL modification was enhanced in the presence of CHER and POE-POB. The above findings suggested that, in the presence of CHER with POE-POB, apo E and apo C-III—which are relatively hydrophilic, of low molecular weight, and rich in VLDLR—were removed, and this phenomenon triggers the modification of VLDLR.

Using postprandial sera with high TGs, there were substantial differences between the immunoseparation method and the reagent with POE-POB in the presence of CHER and CHOD. To determine the cause of discrepancies, postprandial serum was collected from an individual after a high-fat meal. Whereas large CMs were eluted in the void volume during gel filtration by use of a serum sample collected from this individual, lipoprotein fractions containing apo B-48 together with apo E and apo C-III were detected in smaller particles. Although CMs of varying size are secreted postprandially (*1*), the smaller particles include some CMRs, in which TGs and some phospholipids have been hydrolyzed by LPLs. In the presence of CHER and CHOD, the reactivity of POE-POB toward the fractions containing such CMRs was found to be very weak, and this reaction was evidently the cause of the discrepancies. Therefore, in an attempt to improve the reactivity toward CMRs, PL-D was added to the reagent with CHER, CHOD, and POE-POB. The results showed no changes in the reactivity to total cholesterol in lipoproteins other than the fractions containing CMRs, but the reactivity toward cholesterol in these fractions improved significantly. PL-D acts on the phosphodiester bond of the polar area of phospholipids to catalyze hydrolysis (*30*). In the absence of POE-POB, PL-D increased the reactivity of the assay for all lipoprotein fractions, probably through the hydrolysis of phospholipids on the surfaces of all the lipoprotein particles, thereby triggering favorable modification of the particles, allowing detection of its cholesterol in the presence of CHER and CHOD. On the other hand, POE-POB interfered with the ability of lipoprotein cholesterol, with the exception of TRL remnant cholesterol, to participate in the subsequent enzymatic reactions. Therefore, the combination of PL-D and POE-POB seems to increase the reactivity of the assay selectively for CMRs (Fig. 3A).

Lipoproteins are essentially microemulsions in which a hydrophobic core containing nonpolar lipids, such as TG and cholesterol esters, is surrounded by a monolayer of apos and polar lipids, such as phospholipids and free cholesterol (*31*). Remnant lipoproteins are produced when CM and VLDL lipids are hydrolyzed by LPLs. It has been reported that hydrolysis of TGs by LPLs occurs at the same time as removal of polar components on TRL